Mucoadhesive Nanoparticles for Treatment of Influenza A

by

Aaminah Ahmad

A thesis

presented to the University of Waterloo

in fulfilment of the

thesis requirement for the degree of

Master of Applied Science

in

Chemical Engineering (Nanotechnology)

Waterloo, Ontario, Canada, 2017

Author’s Declaration

This thesis consists of material all of which I authored or co-authored: see Statement of Contributions included in the thesis. This is a true copy of the thesis, including any required final revisions, as accepted by my examiners.

I understand that my thesis may be made electronically available to the public.

Statement of Contributions

I would like to state Dr. Shengyan Liu's contributions to the project through his creation of the mucoadhesive nanoparticles for ocular drug delivery. I would also like to state the contributions of Aaron Clasky, Soung-Jae Bong, Erij Elkamel, Sukrit Rajpal, and Aya Tsugimatsu in synthesizing nanoparticles for many of my experiments, and conducting some experiments on my behalf. In this they all contribute to chapters 3 and 4. Parts of chapter 3 are from the publication "Prolonged Ocular Retention of Mucoadhesive Nanoparticle Eye Drop Formulation Enables Treatment of Eye Diseases Using Significantly Reduced Dosage" published in *Molecular* Pharmaceutics of which I am a co-author.

The planning, parameter setting, experimental work, and analysis are my own.

Abstract

Influenza A is the most pandemic-prone class of the influenza virus, with new strains emerging every year. Though vaccination is promoted as the vanguard against wide-spread infection, it is not enough to withstand mutating virus strains. Current antiviral therapeutics are frequently falling to resistant virus types. Better antiviral therapies are needed, and nanotechnology can be part of the solution.

Mucoadhesive nanoparticles (MNPs) are nanoparticles which bind to the mucus membrane. Polymeric micellar MNPs made from poly(lactic acid), dextran, and phenylboronic acid have been quite successful in ocular drug delivery to treat dry-eye disease. Their mucus-binding ability points to applications in treatments for other diseases which target the mucus membrane, such as influenza A.

This thesis aims to determine the potential for MNPs as a new class of antiviral therapeutic. A review of current literature highlights the use of nanoparticles in influenza treatment, and the work in this thesis draws on this information. Binding kinetics studies are conducted to determine the strength of MNPs' binding with mucin/sialic acid, and compare this to that of sialic acid-influenza as found in literature. The effect of aerosolization on the MNPs is studied in terms of their key characteristics such as morphology and drug encapsulation in order to determine their suitability as a delivery vehicle to the pulmonary tract. The binding kinetics studies also provide another avenue of study regarding prediction of *in vivo* mucoadhesion using *in vitro* techniques.

Overall these studies present a promising basis for the use of MNPs as a novel antiviral therapeutic. Through detailed binding kinetics and aerosolization studies, the first *in vitro* steps have been established for their viable use. Further steps involving *in vitro* and *in vivo* studies are discussed in the conclusions.

Acknowledgments

First and foremost I'd like to thank my supervisor Dr. Frank Gu for his guidance and support on this project. I'd also like to thank Dr. Shengyan Liu for his mentorship and creation of the project, along with his direction and support.

Our research group has been an excellent source of aid and solicitude over the last two years. Special thanks to the bio side for all their help, support, and friendship.

Funding for this work came from AmorChem, the University of Waterloo, and the National Sciences and Engineering Research Council of Canada.

Dedication

To my parents and sister. Your love and support carry me through everything.

Table of Contents

List of Figures

List of Tables

List of Equations

List of Abbreviations

In order of appearance

MNPs: mucoadhesive nanoparticles

PLA: poly(lactic acid)

PBA: phenylboronic acid

CsA: cyclosporine A

SA: sialic acid

LSPR: localized surface plasmon resonance

RNP: ribonucleoprotein

HA: hemagglutinin

NA: neuraminidase

M2: matrix ion channel

NPs: nanoparticles

AgNPs: silver nanoparticles

AuNPs: gold nanoparticles

PAMAM: polyamidoamine

PEO-PCL: poly(ethylene oxide)-polycaprolactone

MDCK: madin-darby canine kidney cells

RT-PCR: reverse transcription polymerase chain reaction

TEM: transmission electron microscopy

DLS: dynamic light scattering

EE: encapsulation efficiency

DL: drug loading

MOI: multiplicity of infection

SDS: sodium dodecyl sulfate

Chapter 1. Introduction

1.1. Background

Mucoadhesive nanoparticles (MNPs) are a class of nanoparticles (NPs) which bind to the mucus membrane throughout the body [1]–[3]. Our research group has developed MNPs for targeted drug delivery to the ocular surface [4]. These MNPs are polymeric micelles with a hydrophobic core of poly(lactic acid) (PLA), a hydrophilic shell of dextran, and a corona of phenylboronic acid (PBA) grafted onto the dextran. A schematic is shown in Figure 1.

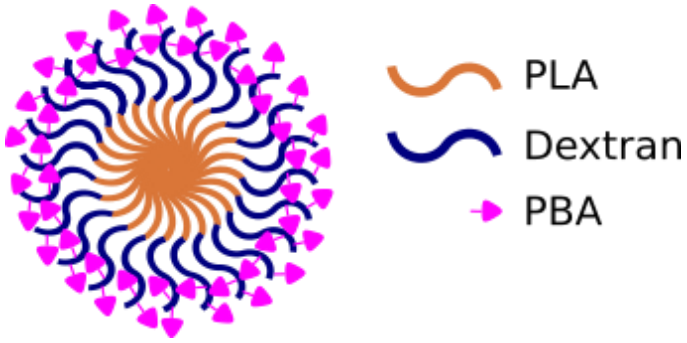

Figure 1. Schematic of MNPs with hydrophobic PLA, hydrophilic dextran, and PBA grafts

The MNPs are currently used for ocular drug delivery to treat dry-eye disease. Cyclosporine A (CsA, the active ingredient in Restasis®) is encapsulated in the hydrophobic interior of the MNPs, and is delivered to the ocular surface by eye drops, as seen in Figure 2.

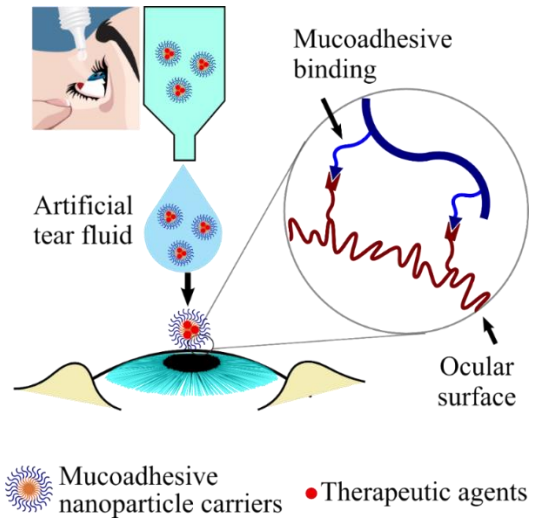

Figure 2. MNP delivery to the ocular surface. Mucoadhesive binding occurs between the MNPs and the surface, allowing it stay and deliver CsA. [4]

The mucoadhesive binding occurs between the PBA grafts on the MNPs and *N*-Acetylneuraminic acid, or sialic acid as it is more often called. Sialic acid (SA) is the terminal monosaccharide on the mucus membrane [5]. The binding is shown in Figure 3.

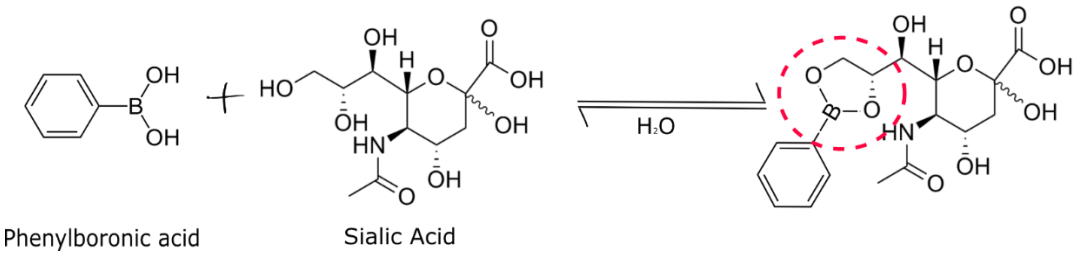

Figure 3. PBA binding to SA

PBA's hydroxyl groups bind to SA through covalent diol-diol binding, allowing the MNPs to stay on the mucus membrane and deliver drugs effectively over a longer period of time than commercial options [4].

As MNPs are quite proficient at binding to the ocular surface, it was hypothesized that their mucoadhesive binding prowess could be applied to other mucus membranes. Mucus membranes protect much of the internal cavities in the human body, varying from the ocular surface to the

gastric surface, to the vaginal surface and more [6]. One such application for MNPs is the pulmonary tract, with its mucus membrane protecting the underlying epithelial cells. The membranes share many features, as seen in Figure 4.

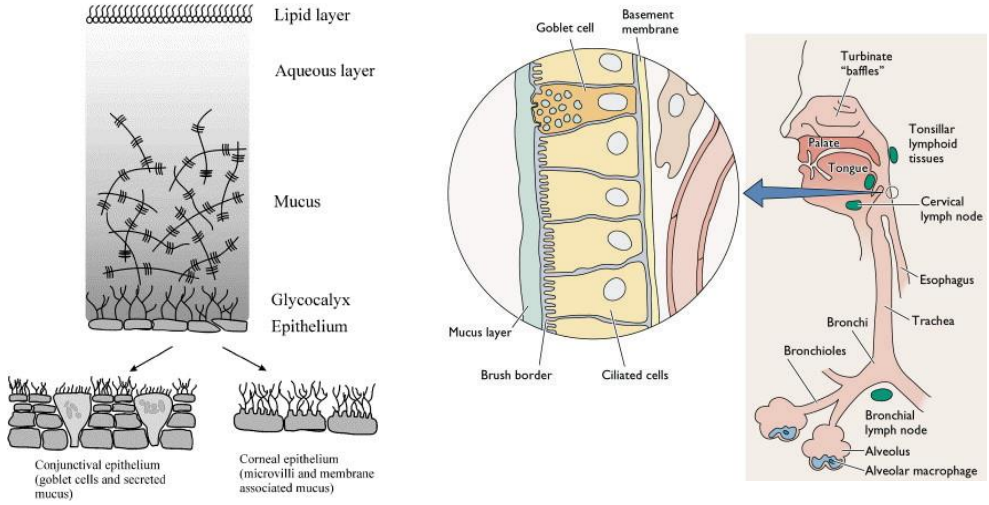

Figure 4. Ocular mucosal membrane (left) compared to pulmonary tract mucosal membrane (right) [116][117]

Both mucus membranes are layered above epithelial cells with goblet cells interspersed throughout, and are made of similar mucin structures with SA as the terminal monosaccharide group [5]. These similarities allow for a comparison of MNPs' ability to bind to the pulmonary tract mucus membrane in a similar vein to its ocular membrane binding, and to be of use in treating diseases which infect this location.

A common illness involving the pulmonary tract is the influenza A virus, which enters the body through inhalation. Influenza A is from the orthomyxovirus family, which consists of viruses composed of a lipid envelope with negative-sense RNA inside, and is responsible for 3 to 5 million infections and 250 000 to 500 000 deaths worldwide annually [7]. With such a large scope, effective prevention and treatment mechanisms are necessary to combat its spread. While vaccines are an important component to influenza care, they are limited in their abilities to treat a broad-

spectrum of viruses as they are specifically designed to inhibit the top contenders for pandemics every year [8], and so are ineffective against the antigenic drift which occurs throughout the season. Current antiviral therapeutics are limited in their efficacy and have spurred resistance among many virus strains to their antiviral mechanisms [9]–[11]. In short, new methods and materials are needed to combat influenza viruses.

MNPs can pave the way for new antiviral treatments by being both a delivery vehicle for drugs, and a steric hindrance for actual influenza virus binding. Influenza infection starts with the binding of the virus particle to SA on the mucus membrane, which is also the target receptor for MNPs. If this binding can be blocked by MNPs while they concurrently deliver antiviral drugs, this will be a new approach to antiviral therapeutics which will minimize the likelihood of resistance cropping up due to the multivalent strategy used.

1.2. Research objectives

The goal of this research was to determine the feasibility of using MNPs for a new application: treatment of the influenza A virus. This was done by:

1. Establishing qualitative binding kinetics studies to compare binding of MNPs vs. control NPs to mucin
2. Defining a straightforward, facile method to determine binding kinetics quantitatively between MNPs and SA and comparing this to influenza-SA from literature
3. Aerosolizing MNPs and determining if they retain similar properties from pre-aerosolization (morphology, encapsulation efficiency, drug release)

1.3. Thesis outline

This thesis is written as follows:

Chapter 1 provides an overview of the thesis itself, along with background on the topic. This serves as a framework for the research presented.

Chapter 2 is an in-depth literature review on the current research into using NPs for treatment of influenza A. The infection mechanism is presented, along with shortcomings in current treatment methods. Silver, gold, metal oxide, and polymeric NPs are reviewed.

Chapter 3 discusses the first step in assessing the viability of MNPs as an antiviral treatment, which is to obtain quality binding kinetics data. Localized surface plasmon resonance (LSPR) acquires real-time binding information between the MNPs and mucin, allowing comparisons to the binding between PLA-Dex NPs (control NPs with no PBA on the surface) and mucin. Data which shows binding with mucin is crucial as this mimics *in vivo* systems more accurately than simply using SA. From there, quantitative binding kinetics data is obtained in the form of the association constant K_A. Fluorescence spectroscopy is used to determine this data. The results are compared to literature values for influenza and SA in order to determine the appropriateness of using MNPs to combat influenza. An off-shoot of these binding kinetics methods was discovered where they can be used to correlate *in vitro* and *in vivo* mucoadhesion of the MNPs. The preliminary data is discussed here.

Chapter 4 delves into aerosolization of the MNPs in preparation for their eventual pulmonary delivery. MNPs' characteristics and properties are examined before and after aerosolization to determine their feasibility in carrying antiviral drugs. Their morphology, encapsulation efficiencies, drug loading, and release capabilities are studied. CsA is encapsulated as a model drug, as it aids with pulmonary function and has previously been encapsulated in MNPs.

Chapter 5 wraps up the research with conclusions and suggestions for future work.

Chapter 2. Literature Review

This review aims to present a comprehensive picture of influenza A treatment with NPs, while framing it in the larger context of the influenza infection mechanism and shortcomings of current antiviral therapeutics. Influenza A is the primary focus of this review, as it is the most wide-spread and harmful variant of influenza for humans, and evolves at a much more rapid rate than influenza B, the other pandemic-causing class of influenza [12][13].

2.1. The influenza A virus

The influenza A virus is a roughly spherical, 80-120 nm particle. It consists of a viral lipid envelope containing ribonucleoproteins (RNPs) made up of the negative-sense genomic RNA which code for the virus proteins and RNA polymerase. There are two major glycoproteins (hemagglutinin and neuraminidase) and matrix ion channels traversing the lipid envelope [14][15]. Hemagglutinin (HA) and neuraminidase (NA) make up the majority of the proteins available on the surface, while the matrix (M2) ion channels appear in a ratio of one M2 channel to approximately 10-100 HA proteins [16]. A detailed image is in Figure 5.

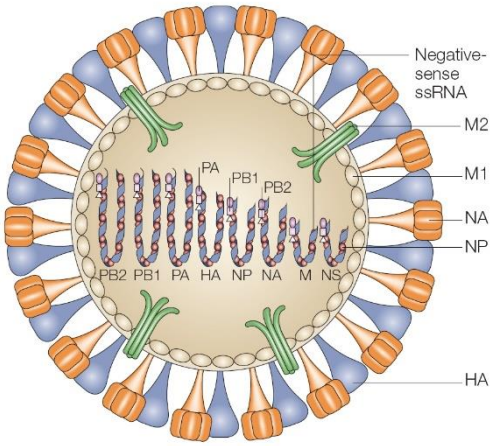

Figure 5. Influenza virus particle [118]

HA and NA present different antigens depending on the virus type, and antibodies can be generated for these specific antigens. Therefore, viruses are classified based off their antigenic types (i.e. H1N1 for the H1 HA, N1 NA protein) [17]. HA is primarily responsible for binding the virus particle to the mucosal membrane and human epithelial cells in the pulmonary tract, whereas NA is responsible for allowing the newly-replicated virions to exit the cell [18]. HA is a trimer with 2 distinct regions, a stem with alpha-helices and a globular head with antiparallel beta sheets. Binding of the virus particle to the mucosal membrane/epithelial cells occurs with the head [19]. NA is a tetramer with a mushroom shape, with a transmembrane stem. It is responsible for cleaving the target receptors from the cells in order to release the budding virions [20]. The M2 ion channel is a tetramer transmembrane protein, and is involved in viral entry into cells via the endosome [21]. There are four main stages to influenza A infection: virus binding to epithelial cells, viral entry into the cell, viral replication within the cell, and virus release outside of the cell [22]. Each stage is elucidated below.

2.1.1. **Virus binding to epithelial cells**

The influenza virus is transmitted person-to-person through either direct contact with an infected person, aerosol inhalation, or indirect contact with a contaminated surface [23]. Upon entry into the pulmonary tract, the virus particles come in contact with the mucosal membrane, and through it, the target epithelial cells.

As mentioned before, HA is the primary component of the virus responsible for binding to the cell membrane. Its target receptor is sialic acid, the terminal monosaccharide present on the cell membrane in epithelial cells [5]. HA binds to SA through hydrophobic interactions and hydrogen bonding with a conserved area of its globular head region [24][25]. The second carbon of SA can be bound to galactose at either its third or sixth carbon, leading to either α-2,3 or α-2,6

linkages. Different HAs prefer to bind to different linkage types, and as α-2,6 is the most prevalent type in human epithelial cells, influenza subtypes with HAs that bind to them are the most common for pandemics in humans [26].

Upon binding, the HA molecule is endocytosed, which causes its cleavage by serine proteases into its two subunits, HA1 and HA2. HA1 is the location of the SA binding site, and HA2 is a fusion peptide which helps with binding to the endosomal membrane [27].

2.1.2. **Viral entry into epithelial cells**

The endocytosis of the virus is dependent on the acidity of the endosomal environment. It is the acidity itself which causes the cleavage of the HA protein discussed in 2.1.1. The HA2 fusion peptide binds the viral envelope to the endosomal membrane, allowing the viral proteins to be released into the cytoplasm of the host epithelial cell [28][29]. The acidic environment is also used for its hydrogen ions which are transferred into the virus particle through the M2 channel. These protons aid with the release of the viral proteins into the host cytoplasm by interfering with inner protein interactions [30].

2.1.3. **Viral replication inside cells**

All influenza RNA replication happens in the host cell nucleus, and so the first objective of the RNPs is to find the nucleus. This is directed by the RNPs' nuclear localization signals [31]. Once in the nucleus, the viral mRNA is polyadenylated and capped to more closely resemble the host cells' mRNA, and it is translated as such [32]. However the resulting RNPs are exported through viral components from the nucleus.

After synthesis of the RNPs, they are packaged into virus particles to create infectious virions. The whole genome of the virus must be incorporated into each virus particle for it to be

fully infectious. Packing signals found on certain RNPs indicate that the viral packaging system is somewhat ordered to create more infectious particles [33][34].

2.1.4. **Viral release**

The newly-created virions bud at the cell membrane, with the virus' M1 matrix playing a role in closing off the budding viruses [35]. HA continues to bind the virions to the SA on the cell membrane until NA cleaves the bonds to release the virions out of the cell, causing apoptosis [20]. NA also increases the infectivity of the new viruses by removing SA from the viral envelope, which helps prevent aggregation [36].

2.2. Challenges in current treatment methods for influenza A

There exist many challenges for the present-day treatment of the influenza A virus. Though vaccination is thought to be the best method of coping with the virus due to its preventative nature, typical influenza vaccines are made to target only specific subtypes of influenza, and so are not effective across the broad spectrum. They also take time to prepare, are not effective in certain demographics of the population, and cannot adapt to antigenic changes in the virus throughout the season [37]. This leaves antiviral therapeutics.

There are two main types of antiviral drugs currently on the market: NA inhibitors and M2 channel inhibitors. The challenge with both is often virus resistance, which will be discussed further below.

2.2.1. **NA inhibitors**

The two main NA inhibitors are oseltamivir (Tamiflu®) and zanamivir (Relenza®). Both work by inactivating the NA protein on the virus particle. This leads to the newly-made virions being unable to release themselves from the host cell, as described earlier. Instead of releasing,

they remain aggregated at the budding points on the cell membrane of the host cell, and thus reduce overall viral infectivity [38].

Antiviral drug resistance is a growing problem, exacerbated by influenza A's high mutational rates. Resistance can come from just one point mutation in a significant location in the M2 or NA protein [39], [40]. Oseltamivir-resistance has begun to grow amongst influenza A strains, most likely due to its common use as an easy-to-administer drug (oral administration) [41]. Generally, influenza A strains which exhibit resistance to oseltamivir are still susceptible to zanamivir, as the most common NA mutation which causes resistance affects the binding site of oseltamivir, not zanamivir [42]. However, zanamivir-resistance has been found in influenza B strains, indicating that it is only a matter of time before this spreads to influenza A [43].

2.2.2. **M2 channel inhibitors**

The two M2 channel inhibitors are amantadine (Symmetrel®) and rimantadine (Flumadine®), which act by blocking the M2 channel. This blockage inhibits viral replication in the host cell, as the M2 channel is used to transfer protons into the cell and fuse the endosomal membrane to the viral envelope, as described earlier.

These drugs have been in use for four decades, and as such are now considered ineffective as when used alone as therapeutics for influenza A due to the high levels of resistance across the virus subtypes [44]. Resistance to one automatically confers resistance to the other, as they have very similar mechanisms of action [45]. It has reached the point where NA inhibitors are considered the only effective antiviral therapeutic, as M2 inhibitors now have worldwide influenza A resistance [46]. Amantadine and rimantadine also have many toxic side-effects, inhibiting their use [47].

2.3. Advantages of NPs

Nanoparticles, as mentioned earlier, are particles with at least one dimension on the nanoscale (10^{-9} m). Particles of this size often display very different properties than their bulk form due to their high surface area to volume ratio. This allows for a large degree of surface functionalization, thus favouring more reactivity with desired targets [48]. In the healthcare field, NPs have been used for drug delivery systems, biosensors, and as a combination of both drugs and delivery vehicle [49]–[51]. Some common advantages of NPs in this field include: high sensitivity and specificity for targets, ability to tune drug release, use lower doses, detect lower concentrations, and reduce costs [52]–[55].

NPs' advantages make them strong candidates for influenza treatment. They can often subvert the restrictions on current antiviral therapies to create multivalent strategies to fighting influenza. Drugs which are toxic on their own can have lessened toxicity when bound to NPs, as lower doses can be used and less of it will travel to areas other than the target. Their size makes them ideal for influenza treatment, as they are likely to settle in the same parts of the pulmonary tract as the influenza virus upon inhalation. They are more suited to do so than microparticles, and are more likely to be retained in the pulmonary tract. In a study with carbon particles and shallow aerosol bolus inhalation in humans, 75% of particles sized <100 nm were retained in the lungs after 24 hourse, while only 10-20% of particles sized between 100 nm and 10 μm remained [56], [57].

NPs for treatment of influenza A can be approached in a variety of methods, from using a NP as the drug itself, to using it as simply a delivery vehicle, to a combination of both. A variety of materials can be used, such as different metals, metal oxides, and polymers. These methods are detailed in the next section. For a summary see Table 1.

Table 1. Summary of current research in NPs for treatment of influenza A

Category	Specific material	Drug	Mechanism	References
AgNPs	AgNPs w/o coating	No drug	AgNPs disrupt viral envelope, destroy virus	[58]–[60][61]
		Oseltamivir, zanamivir	AgNPs disrupt viral envelope, oseltamivir & zanamivir inhibit neuraminidase activity	[62], [63]
		Amantadine	AgNPs disrupt viral envelope, amantadine blocks M2 channel	[64]
AuNPs	SA moieties	No drug	AuNPs acted as scaffold for various sialyllated moieties on the surface, inhibited hemagglutination activities	[65]–[67]
	AuNPs w/o coating	Oseltamivir	Modified oseltamivir and attached to AuNPs, retained inhibitory effects	[68]
Metal Oxides	TiO_2	No drug	TiO2 disrupts viral envelope, destroys virus	[69]
		Deoxyribozymes	TiO2 delivers deoxyribozymes into cells, inhibits viral replication	[70]
	Silicate	No drug	Surfactant-modified nanoclay inhibited viral replicaton	[71]
	Iron oxide	No drug	Glycine-coated iron oxide NPs inhibit antiviral activity	[72]
Polymeric NPs	Dendritic and linear polymeric NPs with SA	No drug	PAMAM dendrimers coated with sialyllactose and linear polyglycerol sialosides both inhibit hemagglutination, destroy virus	[73], [74]
	Polymersome with dendritic branches & SA	zanamivir	PEO-PCL polymersome coated with SA bind well to lectins, encapsulate and release zanamivir	[75]
	Cyclic dextrins with SA	No drug	α-glucuronic acid-linked cyclic dextrins with sialoglycoside outer shell inhibits hemagglutination activities	[76]

2.4. Current use of NPs to treat influenza

2.4.1. Silver NPs

Silver NPs (AgNPs) have been used in antimicrobial applications for some time now, and are excellent for this application due to their multivalent approach as antibiotics [77]. AgNPs' main antimicrobial properties are its ability to leach silver ions, which interfere with bacterial cells and thus destroy them. However AgNPs are also able to interfere with bacteria in their whole particle form, thus creating a two-pronged approach [78]. Using a multivalent strategy limits the ability of the bacteria to gain resistance, and indeed resistance to silver/AgNPs has not yet surfaced among bacteria naturally [79]. The above-mentioned properties make AgNPs an important topic in the study for effective antivirals.

AgNPs have been synthesized in a variety of ways, and used in a plethora of applications [80], [81]. Their antiviral application for influenza A specifically started in 2009 with Mehrbod et al. investigating their antiviral effects *in vitro* [60]. In this paper they determined the cytotoxicity of commercial AgNPs on Madin-Darby Canine Kidney (MDCK) cells to find the appropriate concentration to use on further tests with influenza A. This concentration was 0.5 μg/mL, and this was used in several *in vitro* tests with an H1N1 strain of influenza A. A hemagglutination inhibition assay was performed to check the AgNPs' ability to inhibit the virus with red blood cells. A virus inhibition assay was done with MDCK cells and a colourimetric MTT assay, where confluent MDCK cells were infected with 100 $TCID_{50}$ of the virus, allowed to bind for 1 h, and unbound virus was removed after with a wash. Then 100 μL of AgNPs were diluted with their medium and added to each well. The MTT assay involves the colour-changing ability of the MTT compound. Yellow MTT is changed to purple formazan in the presence of healthy cells due to their mitochondrial activity. If a colour change is not observed, it is assumed that the cells are not

healthy/they are dead [82]. In this case, MTT was added to the cells after the AgNPs, and absorbance values were measured. This showed an increase in cell viability with the addition of the AgNPs compared to virus-only cells, with 58.52% protection. Similar experiments with the additions of AgNPs before virus, and concurrently with virus, showed even higher protections. Other *in vitro* studies such as reverse transcription polymerase chain reaction (RT-PCR) confirmed these results. Merhbod et al. also elucidated the mechanism of AgNPs' antiviral activity, where they estimate that the AgNPs are themselves attacking the disulfide bonds which hold the HA1 and HA2 subunits of HA together. This would block the receptor binding sites on HA, rendering the virus inactive [60].

After this publication, many groups have studied the inhibitory effect of AgNPs on the influenza A virus. Publications generally dealt with *in vitro* tests described above such as the MTT assay, or the hemagglutination inhibition assay. Xiang et al. published papers dealing with naked AgNPs for both H1N1 and H3N2 [61], [83]. H1N1 studies were done only *in vitro*, where flow cytometry was used to determine the post-infection effect of 10 nm AgNPs on MDCK cells. The treatment reduced cell apoptosis by 9% compared to virus-only. Other tests including a hemagglutination inhibition assay showed the inhibitory effect of the AgNPs [83]. H3N2 studies were done both *in vitro* and *in vivo*. *In vitro* tests showed that MDCK cells infected with influenza virus for 2 hours prior to AgNPs being introduced showed an apoptosis rate of 13.58% +/- 4.86%, whereas the control virus-infected cells had a rate of 25.29% +/- 3.66%. *In vivo* tests were conducted with female BALB/c mice which were infected intranasally with 20 μL of H3N2 virus. AgNPs and oseltamivir were administered 24 hours after infection, and three times after to achieve a 5 mg/kg and 2 mg/kg dose of AgNPs and oseltamivir respectively (different groups of animals received different treatments). Mice treated with AgNPs had a 75% survival rate compared to the

control influenza group, and showed a reduction in lung virus titers by more than two orders of magnitude (comparable to the oseltamivir-treated group) [61]. This showed the ability of AgNPs to treat influenza A both *in vitro* and *in vivo*.

As mentioned before, AgNPs have a wide variety of synthesis methods. Plant-based syntheses are growing in popularity for their safer chemistry and ease-of-use [80]. These methods certainly do not detract from the inhibitory effects of AgNPs on influenza, as demonstrated by Fatima et al. [59]. Cinnamon powder was used as the reducing agent, and their resulting AgNPs showed no significant toxic effects on Vero cells (up to 500 μg/mL). Both the cinnamon extract and the AgNPs were tested for their influenza inhibiting effects. Vero cells were infected with 10^4 $TCID_{50}$ and incubated for 2 hours. After this, unbound virus was removed and 100 μL of cinnamon extract or the AgNPs were added at varying concentrations. Cells were further incubated for 48 h, after which the MTT assay was carried out. A dose-dependence was established with the AgNPs, and at 200 μg/mL, the infection level of the cells was decreased to below 40%, compared to the 100% of the virus-control cells.

Apart from naked AgNPs, drug-AgNP conjugates have been tested for their efficacy. It is thought that synergistic effects could be found by combining common antiviral drugs with AgNPs, which here would act as both a delivery mechanism and a therapeutic. This is thought to be one method to avoid antiviral resistance, where using a multivalent approach can help. Three major antiviral drugs have been tested this way: oseltamivir (Ag@OTV), zanamivir (Ag@ZNV), and amantadine (Ag@AM) [62]–[64]. All three publications involved adhering the drug to the surface of AgNPs, though the chemistry is not explained. A number of *in vitro* tests were conducted, including hemagglutination inhibition assays, neuraminidase inhibitions assays, and MTT assays for cell viability. The neuraminidase inhibition assay was used specifically because oseltamivir

and zanamivir are neuraminidase inhibitors. All three publications had a drug-AgNP conjugate of 2 nm in diameter, which was easily uptaken by cells. MTT assays were conducted with MDCK cells infected with H1N1 virus for 2 hours before washing off unbound virus and adding different concentrations of drug, regular AgNPs, or drug-AgNP conjugates for 24 hours. After this the MTT assay was conducted. Influenza-infected cells had a viability between 36-39%, AgNPs alone had 61-65%, and amantadine, oseltamivir, and zanamivir had 56%, 59%, and 63% respectively. The combination therapies increased the viabilities drastically, with Ag@AM, Ag@OTV, and Ag@ZNV resulting in 90%, 90%, and 82.26% respectively. The therapies with drug-AgNP conjugates had strong results due to their multivalent approach to antiviral therapy. These papers also specify how the drug-AgNP conjugates are able to reduce the generation of reactive oxygen species, which is increased in influenza A-infected cells. They were also able to "rescue" cells from virus-induced apoptosis [62]–[64]. The results indicate an interesting future for these drug-AgNP conjugates.

In general, the AgNP field has come the farthest in antiviral therapies for influenza A, as it has seen some *in vivo* studies for treatment. More needs to be done in the *in vivo* area to continue this line of work.

2.4.2. **Gold NPs**

Gold NPs (AuNPs) have been used in a variety of applications, from detection, to drug delivery, and many others [84]–[86]. They are well-known to be biocompatible and non-toxic, and as such, are often used for biomedical applications. Their use in antivirals is primarily as a scaffold upon which specific receptors can be bound to inhibit the influenza A virus, generally a version of SA. This is because the actual receptor of the HA protein on the virus is SA on epithelial cells, and so NPs with SA and Sa-like surface modifications are likely to be able to inhibit the virus. This

class of antiviral treatment has not come as far as that of AgNPs, where *in vivo* studies have been done, as well as multiple *in vitro* studies with treatment being a primary model. Many of the publications discussed below deal only with inhibition studies, though they are a promising first step to delivering AuNP-antiviral therapies for the future. AuNPs are currently used for a variety of applications [87]–[89].

The first study to look at the inhibitory effects of AuNP-mediated therapeutics for influenza A was by Papp et al., where 14 nm AuNPs were functionalized with glycerol dendrons with SA as the terminal groups [67]. The dendrons were covalently attached to the AuNPs by a thiol group, and two versions were made for testing; one with SA as the terminal group, and one with diol terminal groups. Their interaction with viral proteins such as HA was imaged by transmission electron microscopy (TEM), displaying multivalent binding. The cytotoxicity of the AuNPs was measured with a fluorescence staining test, where 100% viability was maintained in the tested MDCK cells compared to the control. A hemagglutination inhibition assay was conducted with red blood cells, and the functionalized AuNPs' ability to inhibit viral infection was tested with a viral nucleoprotein assay. For this test, the H3N2 virus was incubated with the AuNPs with both SA and diol-terminated groups for 30 min, after which MDCK cells were exposed to the mixture at a multiplicity of infection (MOI) of 25 for five hours. Flow cytometry was used to determine the level of viral nucleoprotein in each sample, which is indicative of viral infection (higher amounts of protein correspond to higher levels of infection). The SA-AuNP sample reduced the infection by 40% compared to the virus-only control, while the diol-AuNP sample showed only a 20% reduction [67]. This was the first conclusive evidence where AuNPs were used in a therapeutic for influenza A.

Since then a few papers have also looked at different methods to introduce SA groups onto AuNPs and study their effects on the influenza A virus. Zhang et al. used reversible addition-fragmentation chain transfer to attach SA to their 17 nm AuNPs with a thiol group [65]. This inhibitor was tested for its ability to bind to different lectins which were representative of HA, and then its ability to bind to H1N1 influenza virions specifically. Dynamic light scattering (DLS) was used to characterize the sizes of the compounds while TEM visualized the binding. TEM showed the specificity of binding between the virus and the SA-terminated AuNPs, compared to a lactose-terminated control. Lectin binding was shown through DLS, where different sizes described different compounds. Inhibition was reported in the cases of SA-AuNPs compared to the lactose control [65]. Feng et al. described a method to introduce thiosialosides onto AuNPs and other metals, where the oxygen of the glycoside bond of the sialoside was replaced by a sulfur group [66]. This prevents interaction of the SA acid with NA, which would try to cleave it off otherwise. The formulations with the highest inhibitory activity for H1N1 were a 20 nm AuNP with 9.8 μM SA on it (hemagglutination inhibition titre of 64) and a 50 nm AgNP with 13.7 μM SA (hemagglutination inhibition titre of 128) [66].

A last example of using AuNPs for antiviral work utilizes oseltamivir in conjunction with AuNPs to create "TamiGold" [68]. Stanley et al. decorated the surface of 2 and 14 nm AuNPs with a modified oseltamivir carboxylate form (oseltamivir phosphonate), which retains similar inhibitory activity to the drug itself. The 14 nm version was simply used for TEM studies to show interaction with the inactivated H1N1 virus, whereas the 2 nm version was used to check inhibitory effects with a neuraminidase inhibition assay (as oseltamivir binds to the neuraminidase protein). IC_{50} values were calculated for the 2 nm TamiGold from the inhibition assay, with 14.7 nM and 12.3 nM for 2 oseltamivir-sensitive strains and 5.3 μM and 14.1 μM for oseltamivir-resistant

strains. These concentrations are the minimum concentrations of oseltamivir phosphonate needed to inhibit the virus. Control samples made with methylphosphonate AuNPs instead of oseltamivir phosphonate showed no inhibitory effects, ruling out unspecific binding [68].

Overall, AuNPs have been shown to provide a versatile scaffold for carrying other therapeutics to treat influenza A. Their biocompatibility and biodegradability make them ideal for targeted drug delivery, and their size and customizability for functionalization make them ideal for influenza A treatment. Current options have progressed very far even by *in vitro* standards, with inhibition being the majority of the tests. Further work with live viruses and cells is needed to determine the therapeutic effect of the AuNP-delivered treatments. Eventually *in vivo* work must be done to further prove the underlying claims from inhibition studies.

2.4.3. **Metal oxide NPs**

Apart from metals, there are many other bases for NP formulations. Metal oxides have seen increasing popularity for biomedical applications. In their bulk form, these metal oxides are often toxic to humans. However when nanoscale versions are used at low concentrations, metal oxides such as TiO_2, ZnO, and SiO_2 have seen success in a variety of therapies [90]–[92].

Naked TiO_2 has been studied for its antiviral properties by Mazurkova et al. [69]. Tests were done to see if TiO_2 was able to inhibit the influenza A virus through a mechanism that did not involve its photocatalytic abilities. H3N2 at a concentration of 9.5 lg $TCID_{50}$/mL was mixed with TiO_2 NPs (4-10 nm) and incubated for different time periods. Increased incubation time led to more destruction of the viral envelope, as seen by TEM. The inhibition effect was seen by adding the TiO_2 NP-influenza mixture to MDCK cells and doing a hemagglutination assay with chicken red blood cells 20 hours after incubation. The inhibitory activity of the TiO_2 NPs was largest at 2 and 7 mg/mL (equal in both, showing a plateau), and was seen irrespective of the lighting

conditions (ultraviolet, daylight, or dark). With both concentrations, the virus titer was reduced from over 6 lg $TCID_{50}$/mL to 0 lg $TCID_{50}$/mL. This antiviral effect of TiO_2 is attributed to its ability to penetrate and destroy the viral envelope, as it is a lipoprotein membrane similar to that of eukaryotic cells, which TiO_2 can enter fairly easily. Low concentrations will have to be used so as to not have adverse effects on non-target cells [69].

Metal oxides as carriers for nucleic acid therapies are an interesting combination, as they may be able to take advantage of the carrier being therapeutic as well (similar to AgNPs from before). Deoxyribozymes are a class of nucleic acid therapeutics which can cleave complementary RNA strands irreversibly, thereby acting as a gene silencer [93]. Repkova et al. studied the effects of coupling deoxyribozymes non-covalently to TiO_2 NPs coated with polylysine to create a nanocomposite. Antiviral efficacy of the nanocomposite was assessed with MDCK cells infected with H5N1 at a MOI of 0.1. Treatment of these cells with the nanocomposite resulted in inhibition by a factor of approximately 3000, which was an order of magnitude higher than the control delivery vehicle lipofectamine. Inhibition was measured by viral titer measurements after treatment with the nanocomposite and control [70].

Kumar et al. looked at the antiviral effects of glycine-coated iron oxide NPs [72]. *In vitro* studies including plaque inhibition assays, RT-PCR, and MTT assays were conducted. Treatment with the NPs within 24 hours of infection of MA104 cells by a 0.5 MOI of H1N1 resulted in an 8-fold reduction of viral RNA [72].

Liang et al. went a different route, investigating the antiviral potency of exfoliated montmorillonite clay [71]. The fully exfoliated clay was called nanoscale silicate platelets, and was coated with sodium dodecyl sulfate (SDS), an anionic surfactant to create NSQc. The addition of the surfactant served to lessen the cytotoxicity of the nanoclay. NSQc was found to have

inhibitory properties for multiple virus types (Japanese encephalitis, dengue) along with influenza. Plaque-formation assays were conducted where the H1N1 virus was mixed with NSQc, along with other versions with different surfactant amounts, then added to BHK-21 cells. Unbound virus particles were washed off after 2 hours of incubation, then agarose-containing medium was laid over the cells for 4 days. Crystal-violet stain was used to determine plaque growth. NSQc and NSQc(A30) showed high inhibitory effects, where the viral titer was reduced by an order of magnitude (A30 had a 70:30 ratio of surfactant to platelets). NSQc(A50) showed no inhibitory effects, from which it can be derived that the surfactant played a major role in antiviral inhibition (A50 had a 50:50 ratio of surfactant to platelets). The main mechanism of action is thought to be the electrostatic interactions between the negative surfactant SDS on the nanoscale platelet, and the positively charged viral envelopes of the viruses studied [71].

Metal oxides display an interesting combination of therapeutic-delivery vehicle/sole therapeutic. TiO2 has been studied *in vitro* fairly extensively for its inhibitory effects and ability to treat influenza A in infected cells. As long as cytotoxicity is kept in check, future work *in vivo* could expand the field greatly. Some new players include the nanoclay and iron oxide NPs, still more in their infancy. Further *in vitro* work is warranted before stepping into *in vivo*.

2.4.4. **Polymeric NPs**

Polymeric NPs have been used for drug delivery in a variety of forms, including micellar, dendrimer, linear, and many others [94]–[96]. Their high degree of customizability allows the use of biodegradable materials and targeting ligands which can allow for smooth delivery with few toxic side-effects.

Dendrimers are a specific class of polymeric NP with branched chains growing out of a core. The therapeutic component can either be non-covalently bonded at the core or on the surface,

waiting to be released once at the target site, or it can be covalently bonded with stable bonds, which could be cleaved upon reaching the desired location, or used to attach the whole dendrimer and employ steric hindrance [97], [98]. Kwon et al. created a polyamidoamine (PAMAM) dendrimer with multivalent properties due to its functionalization with 6'sialyllactose [73]. They performed a number of *in vitro* studies to test its inhibitory effect against the H1N1 virus. The dendrimer was pre-mixed with the virus before addition to MDCK cells, after which ELISA was conducted to determine the IC_{50}. In general, highly-branched versions of the dendrimer with specific spacing requirements showed increased inhibitory activity (3.4 μM was the lowest IC_{50} achieved). Surface plasmon resonance was used to determine the binding between the HA trimer and the dendrimer. *In vivo* studies were conducted for a prevention-type system, where the dendrimers were administered intranasally to mice before infection. Lung viral titer was lower with the dendrimer administration compared to the control, though this is more a prevention aspect [73]. Another study using dendritic branches comes from Nazemi et al., who created a polymersome made of poly(ethylene oxide)-polycaprolactone (PEO-PCL) with sialiodendrons (dendritic branches with SA-terminal groups) [75]. The resulting compound has a two-pronged approach, where the outer shell of the polymersome can bind to HA through the SA, and the inner core can encapsulate an antiviral drug and carry it to the target site. They chose to incorporate zanamivir, and tested the ability of the compound to bind to the *Limax flavus* lectin (similar to HA) and encapsulate and release zanamivir. The entire dendritic-polymersome compound resulted in a 2000-fold increase in binding affinity compared to simply SA. This study is still in the early stages, but there is promise for its multivalent approach to inhibiting influenza.

On the other side, Bhatia el at have created a linear polyglycerol sialoside which performs far better than its dendritic sister [74]. Multiple *in vitro* experiments were conducted in order to

determine the inhibitory performance of each type, both linear and dendritic. Cell viability was conducted with MDCK II cells to determine the cytotoxicity of the compounds (insignificant). Hemagglutination inhibition assays, infection inhibition assays, viral nucleoprotein assays, and others were conducted to show the inhibitory effects of the linear vs. dendritic polysialosides. Most of the studies were conducted with pre-incubation of the virus (H3N2) and polysialoside together before addition to MDCK cells. However one experiment was conducted with infection of MDCK cells (MOI 0.01) with H3N2 and H7N1 for 45 mins before addition of the polysialoside. The linear polysialoside reduced the viral titer by 4 orders of magnitude compared to 3 for the dendritic version. Further studies were conducted *in vivo* as well, but in a preventative measure (samples were administered before virus infection) [74]. This study shows an interesting example of when linear polymeric NPs can perform better than their dendritic counterparts, though most studies discussed earlier show the opposite.

Finally, another example of SA-functionalized NPs comes in the form of α-glucuronic acid-linked cyclic dextrins by Ogata et al. [76]. The backbone of the NP consists of cyclic dextrins with highly branched α-glucuronic acid and sialoglycoside groups on the outer shell. The dextrins offer a high degree of functionalization (allowing for multivalent binding), biocompatibility due to their makeup from sugars, and high aqueous solubility [99]. A hemagglutination inhibition assay was conducted to determine the minimum inhibitory concentration required to completely inhibit hemagglutination with red blood cells. The compound was tested with different amounts of sialoglycoside groups, and it was found that the sample with the highest amounts of SA on the outside inhibited hemagglutination with the lowest concentration (0.09 nM), about 240-fold better than fetuin which also binds well to the influenza virus [76]. This study is still in its infancy, as

only inhibition tests with erythrocytes have been conducted, but the results are promising for future *in vitro* and *in vivo* tests.

Polymeric NPs, through their many attractive properties, have been extensively studied for drug delivery in humans. Much of this can extend to influenza A treatment, where the polymeric NPs range from acting simply as a drug delivery vehicle, to being a scaffold for physical blocking, to a combination therapy of both. Generally this field has not been fully studied in terms of influenza A treatment; more *in vitro* and *in vivo* studies can be done to ensure effectiveness. Linear vs dendritic NPs have traditionally gone in favour of dendritic for their inhibitory effects, though as seen above this is not always the case. More study is generally needed in this field.

2.5. Conclusions/Outlook

Influenza A is a growing problem, with pandemics, antiviral resistance, and new strains appearing every year. Current therapies either have already failed (M2 channel inhibitors) or are showing signs of imminent failure (neuraminidase inhibitors) in the solo treatment approach. New methods are needed to properly treat influenza A, and NPs can be a major component of the solution. From metals to metal oxides, to polymeric and beyond, NPs are able to transcend typical therapeutic limitations due to their size, surface-functionalization abilities, and multivalent approaches to treatment (sometimes acting as both carrier and therapeutic). AgNPs show this characteristic quite well, where the antibacterial effects are able to carry over to antiviral (though through a different mechanism). AuNPs act as an excellent scaffold, often for SA moieties. Metal oxides can combine both vehicle and therapeutic at times. Polymeric NPs can deliver treatment/act as a scaffold for blocking, similar to AuNPs. Overall the AgNP field has come the farthest in starting *in vivo* studies, though this may be because the antibacterial properties had been well studied beforehand. The other fields have different *in vitro* studies, though some only come as far

as inhibition as opposed to treatment. Polymeric NPs, with their biocompatibility, biodegradability, and ability to utilize a multivalent approach to combatting influenza, are a field worthy of further exploration.

Chapter 3. Establishing binding kinetics of MNPs

3.1. Determination methods

As seen in section 2.4, one of the typical first-steps in establishing the inhibitory effects of a possible antiviral compound is determining the binding kinetics between said compound and hemagglutinin, or conducting a hemagglutination inhibition assay. Though this is a straightforward method for many studies, it is not possible to use for the MNPs' novel proposed method for antiviral activity. This is because MNPs bind specifically to the SAs on the mucus membrane (through mucoadhesion), and by doing so can block the binding of the virus and deliver antiviral drugs. They do not affect the virus' ability to hemagglutinate red blood cells, as they do not bind to the HA protein. Therefore, new methods were needed to determine the binding abilities of the MNPs, and compare them to that of influenza.

Mucoadhesion has been measured through a variety of methods throughout the years. Using sheep mucus strips, Swamy et al. measured how many of their particles remained bound to the strips after a wash and calculated percent mucoadhesion [100]. Chary et al. measured the force needed to detach their mucoadhesive polymers from sheep intestines [101]. Lim et al. measured the mucociliary transport rate of their particles on frog palates, and calculated a value in relation to graphite particles [102]. These methods all require specialized materials such as animal organs, and do not measure a direct binding constant. Springsteen et al. measured an indirect binding constant using a three-component fluorescence system, but used a fairly complicated method of analysis [103]. The processes mentioned above do not fit the requirements for the needed tests, which are to calculate a direct binding constant to compare for influenza-SA, and to use a facile method. These conditions can be met by a combination of LSPR and fluorescence studies with rigorous design parameters.

First, LSPR was used to observe the real-time binding of MNPs to mucin, and compare this to PLA-Dex NPs (control samples with no PBA on them). This is an *in vitro* test which validates the PBA as the mucoadhesive component of the MNPs. Mucin is used to more accurately mimic *in vivo* studies. Many iterations and parameters were studied for this test before the design reported below was finalized.

After the qualitative studies with LSPR were conducted, quantitative studies were needed to establish a binding constant value for MNPs with SA to be able to compare to literature values of influenza-SA. The SA-hemagglutinin dissociation constant has been widely studied, and found to be 2-3 mM [104], [105]. This translates to a K_A of approximately 333-500 M^{-1}. Therefore in order to be a competent antiviral therapeutic, the MNPs would need a binding constant >500 M^{-1} with SA. This is covered by fluorescence studies.

While fluorescence studies were underway for determining binding constants, it was noticed that this same study could be used for an *in vitro* test as a predictor of mucoadhesion *in vivo*. The theory was that lower amounts of PBA conjugation would decrease mucoadhesion of the MNPs. By changing the amount of PBA on the MNPs, the binding constant value would change proportionally. A study was developed (with preliminary data) which uses both LSPR and fluorescence as a means to predict mucoadhesion, which could be applied to minimize *in vivo* studies in the future.

3.2. Materials and methods

3.2.1. Materials

Acid-terminated PLA (MW: 20 kDa) was purchased from Lakeshore Biomaterials (USA) and washed with methanol to remove monomer impurities. Dextran (MW: 10 kDa), 3-Aminophenylboronic acid monohydrate (PBA), sodium periodate ($NaIO_4$), glycerol, sodium

cyanoborohydride ($NaCNBH_3$), N-acetylneuraminic acid (SA), bovine submaxillary mucin, and CsA were purchased from Sigma Aldrich (Canada). LSPR sensor chips were purchased from Nicoya Lifesciences (Canada).

3.2.2. **MNP preparation**

The amphiphilic block copolymer PLA-Dex was prepared using a previously reported method [106]. NPs were formed by self-assembly of the amphiphilic block copolymer through nanoprecipitation, after which they were surface-modified with PBA in two steps: the hydroxyl groups of the dextran surface of the NPs were oxidized in the presence of $NaIO_4$, and the aldehyde groups were then reacted with the amino groups of PBA using reductive amination in the presence of $NaBH_3CN$[106]. The size of the resulting MNPs was measured by dynamic light scattering (DLS).

MNPs with different mol% of PBA on the dextran monomer were fabricated for the correlating *in vitro* & *in vivo* mucoadhesion study. Initial PBA amounts of 0, 10, 20, and 40 mg were used.

3.2.3. **LSPR Studies**

The binding of the MNPs to mucin was qualitatively measured by LSPR on an OpenSPR system (Nicoya Lifesciences). LSPR is a phenomenon of AuNPs (as well as other materials), where the intrinsic resonance of the AuNPs can shift when they are coated with a substance. Optical measurements can be taken when light is shone on the AuNPs, and these measurements increase upon coating of the AuNPs. This increase can be used to determine binding kinetics between various receptors and ligands [107]. This was used to qualify in real-time the binding between MNPs and control PLA-Dex NPs with mucin, and compare the two. To this end, 100-nm AuNP sensors were purchased and cleaned by successive rinses of deionized (DI) water, ethanol,

acetone, and isopropanol, before being dried with nitrogen gas. DI water was used as the running buffer throughout the experiment, flowing over the sensor surface at 20 μL/min. Bovine submaxillary mucin was dissolved at 10 mg/mL in DI water and vortexed for five minutes. 200 μL of the mucin mixture was injected onto the sensor surface in the OpenSPR at 20 μL/min for 15 min to ensure even coating. 200 μL of 1 mM sodium hydroxide (NaOH) was injected three times after the mucin injection to remove unbound mucin from the surface, after which the injection port was cleaned with DI water and purged with air. After a stable baseline was reached, 200 μL of MNPs or control PLA-Dex NPs was injected onto the sensor surface at 20 μL/min for 5 min, after which the injection port was cleaned with DI and purged with air. The mucin surface was regenerated after each sample injection by injecting 200 μL of 1 mM NaOH onto the surface to remove the samples.

3.2.4. **Fluorescence studies**

To quantitatively evaluate the mucoadhesive properties of MNPs, the covalent interaction between the PBA grafts on the surface of the MNPs and SA molecules was studied. The covalent complexation between PBA and SA quenches the intrinsic fluorescence of the PBA molecules. Thus, the interaction between PBA and SA can be quantified by analysing the relative fluorescence intensities of MNPs in the presence of varying concentrations of SA. The relative fluorescence data can then be analysed to determine the Stern-Volmer binding constant, $K_{SV,}$ using the Stern-Volmer equation as seen in Equation 1 [108],

$$I_0/I = 1 + K_{SV} \times [Q]$$

Equation 1: Stern-Volmer equation

where I_0 is the fluorescence intensity of the MNPs sample without SA ([SA] = 0 mM), I is the fluorescence intensity of MNPs with SA, and [Q] is the concentration of the quenching agent, SA. The K_{SV} value is determined by calculating the slope of the linear fit.

This method was first verified by measuring the K_{SV} of free PBA and SA for comparison with literature values. PBA solutions in DI water were mixed with SA to achieve a constant final concentration of PBA (10 μM) with varying SA concentrations (0, 1, 5, 10, 25, and 50 mM). The mixtures were vortexed for 30 seconds before measurement in a spectrofluorometer (type LS-100, Photon Technology International, Canada). The samples were excited at 298 nm, and the emission scan from 310 to 450 nm was obtained for each sample. The relative fluorescence data was then analyzed to determine K_{SV} using the Stern-Volmer equation. The resulting K_{SV} was compared to K_A values for PBA-SA from literature for confirmation of the method's validity for measurement of MNPs-SA.

After the initial fluorescence study, the experiment was repeated with MNPs. MNP suspensions were mixed with SA solutions to achieve a constant final concentration of MNPs (50 μg/ml) with varying SA concentrations (0, 0.01, 0.02, 0.04, 0.08, 0.12, 0.16, and 0.32 mM). The mixtures were vortexed for 30 seconds before measurement, with the same parameters used. The relative fluorescence data was then analyzed to determine K_{SV} using the Stern-Volmer equation.

3.3. Results & Discussion

3.3.1. MNP characterization

The MNPs were fabricated with 46.1 ± 0.001 mol % of PBA on the dextran monomer. The diameter of the MNPs was 50.2 ± 0.6 nm, while the control PLA-Dex NPs was 60.5 ± 0.9 nm. This diameter is well-suited for pulmonary applications, as it is less likely to be cleared quickly by mucociliary clearance as mentioned earlier.

3.3.2. **LSPR study**

MNPs and control NPs were injected at 0.3 mg/mL onto the mucin-coated surface of the AuNP sensor for five minutes. The resulting changes in signal are shown in Figure 6.

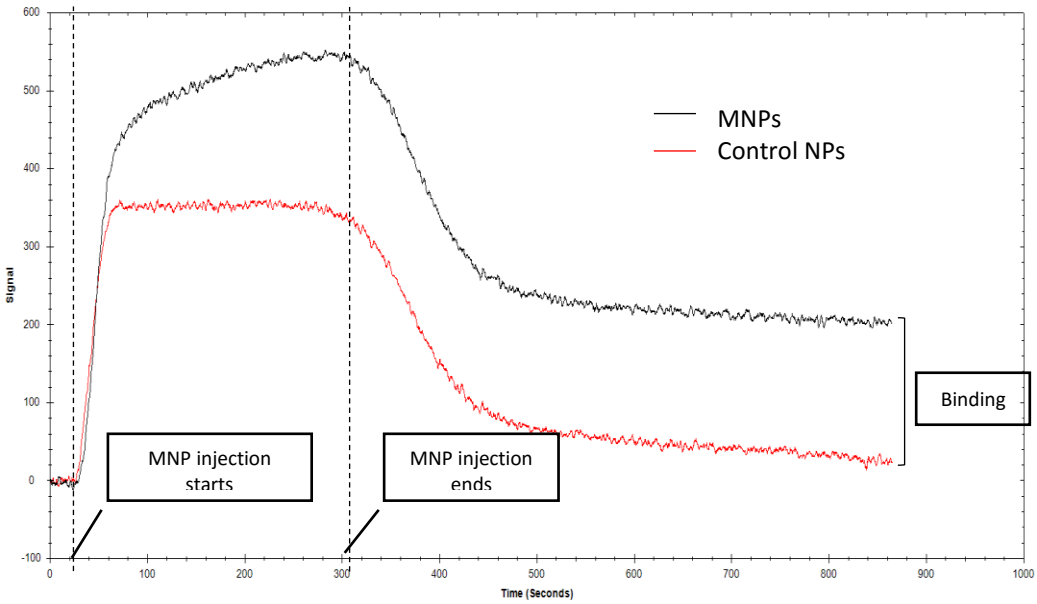

Figure 6. MNP binding (black) on a bovine submaxillary mucin-coated AuNP surface, compared to control NP (red) binding.

Both samples show similar binding curves initially, where the signal increases sharply due to the addition of a new substance onto the sensor surface, regardless of its binding ability. After the initial increase however, changes can be seen. The MNP sample continues to increase throughout the duration of the injection, albeit less sharply than before. This shows that more of the sample is binding to the mucin surface throughout the injection. The control NP sample remains steady for the duration of the injection, showing that though sample is being continually added to the surface, it is not being retained by the mucin coating. Finally after the end of the injection, both samples see a decrease in the signal. The MNP sample steadies itself at a higher baseline than the control NP sample, which returns to close to 0 (where it was at prior to the injection). This means that the

MNP sample has bound to the mucin surface, as the alteration in the baseline signal is both steady and higher than the initial level prior to injection.

Studies involving mucin are very important to be able to more closely mimic *in vivo* conditions. Mucin is the largest component of the mucus membrane, and is made up of high molecular weight glycoproteins with sialic acid as the terminal residue. Bovine submaxillary mucin is an easy-to-obtain source of mucin which is similar to mucin found in pulmonary systems. This study definitively shows the PBA as the source of mucin-binding for the MNPs, gives a real-time window into binding in a more qualitative manner, and does so in a more accurate *in vitro* setting.

3.3.3. **Initial fluorescence study**

The Stern-Volmer method described above was tested for its efficacy in determining an accurate binding constant between PBA-SA before it was used for the MNPs. The emission spectra and analysis are shown in Figure 7.

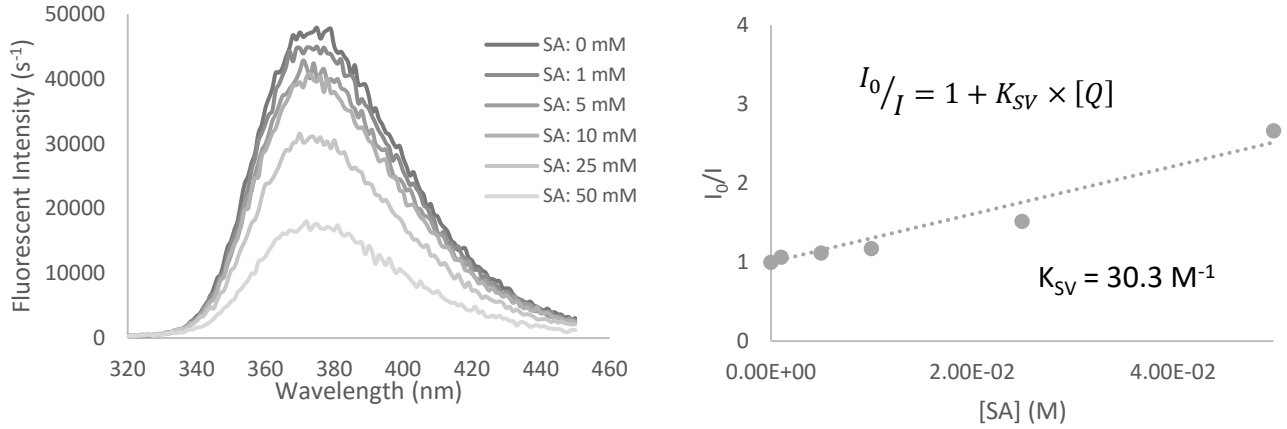

Figure 7. In vitro interaction between PBA and SA. Emission spectra of PBA (50 μg/mL) with various concentrations of SA (0 to 50 mM) at room temperature, λex = 298 nm (left). Relative fluorescence as a function of SA concentrations. I_0 and I represent the fluorescence intensity in the absence and presence of SA respectively. Data were fit according to the Stern−Volmer Equation (right)

The emission spectra on the left show decreasing fluorescence intensity with increasing SA concentrations, as expected for SA's quenching abilities. Further concentrations of SA were not used as the compound had reached a saturation point (see section 3.3.4 for more details). I_0/I vs. [SA] was plotted for every SA concentration used, as shown in the graph on the right. Linear regression was used to fit the data to the Stern-Volmer equation, which gave a K_{SV} value of 30.3 M^{-1}. Literature values place the K_A for PBA-SA between 11.4 M^{-1} – 37.6 M^{-1} depending on the method used to determine it [109], [103], [110]. K_{SV} is known as a binding constant, though depending on the type of fluorescence quenching occurring, it can represent different constants. Static quenching (when the quencher inhibits the excited state from being formed, through a covalent bond for example) yields a K_{SV} which is equal to K_A, the association constant. Dynamic quenching (when the quencher interferes with the excited state after formation) yields a K_{SV} which is its own binding constant, similar but not equivalent to K_A [108]. The PBA-SA quenching occurs through photoinduced electron transfer, where the electron excited in the PBA is transferred to SA instead of being emitted. This is static quenching, and this allows comparisons between the K_{SV} value determined from this method and the literature sources of K_A for PBA-SA binding [111], [112]. The value obtained here (30.3 M^{-1}) is quite comparable with those reported in literature, and as such validates this method for use with MNPs and SA.

3.3.4. **MNPs fluorescence K_{SV}**

Upon validation of the fluorescence method with PBA-SA, the same experiment was conducted for MNPs-SA to determine their K_A. The emission spectra and resulting data analysis are shown in Figure 8.

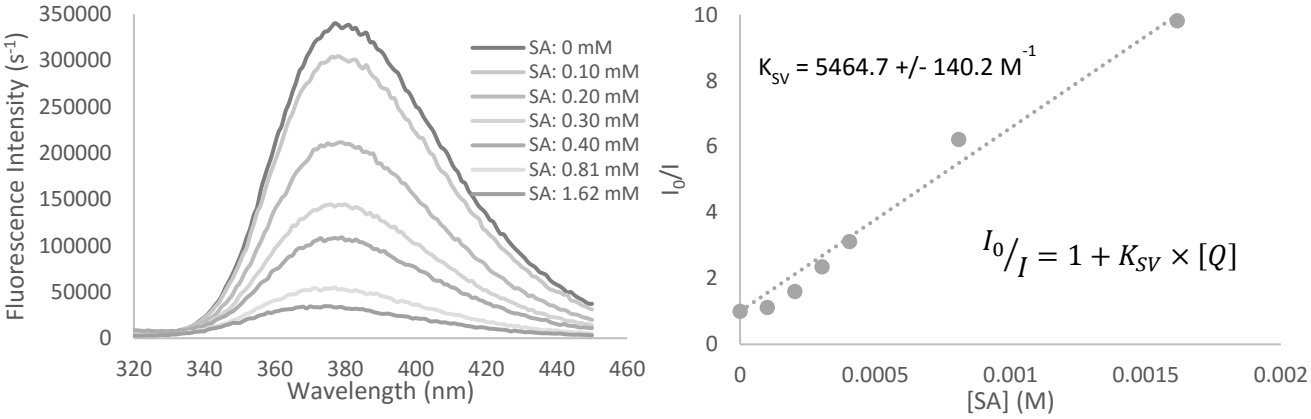

Figure 8. In vitro interaction between MNPs and SA. Emission spectra of MNPs (50 μg/mL) with various concentrations of SA (0 to 1.62 mM) at room temperature, λex = 298 nm (left). Relative fluorescence as a function of SA concentrations. I_0 and I represent the fluorescence intensity in the absence and presence of SA respectively. Data were fit according to the

The emission spectra (left) show decreasing fluorescence intensity with increasing SA concentrations as expected. Further concentrations were not used as the compound had reached a saturation point. I_0/I vs [SA] was plotted for each SA concentration, and the data was fit to the Stern-Volmer equation through linear regression. This yielded a K_{SV} (=K_A) value of 5646.7 +/- 140.2 M^{-1}. This is a very high value for K_A, much higher than what has been previously reported for PBA and PBA compounds with SA. This is likely due to the high number of PBA molecules decorating the surface of the MNPs. Previous PBA compounds which measure the K_A with sialic acid typically have only one PBA moiety per compound [108], [110], whereas MNPs have a high number (15.2 mol% on the dextran monomer). This makes MNPs much more likely to bind to SA, as they have more binding sites available per nanoparticle. This is promising proof for MNPs' ability to target influenza, as the typical SA-HA bond has a K_A ranging from 333 – 500 M^{-1}. MNPs' order-of-magnitude higher K_A vouches for their ability to bind to the mucus membrane much more strongly than the influenza virus, and likely prevent the virus' binding through steric hindrance.

A note on saturation points mentioned above: the analysis for K_{SV} ends at the SA concentration after which the MNP solution becomes saturated with quencher (i.e. adding more quencher does not change the fluorescence intensity by much). If concentrations of SA above the saturation point are used, linear regression is not accurate and the resulting K_{SV} value is very different. This is shown in Figure 9.

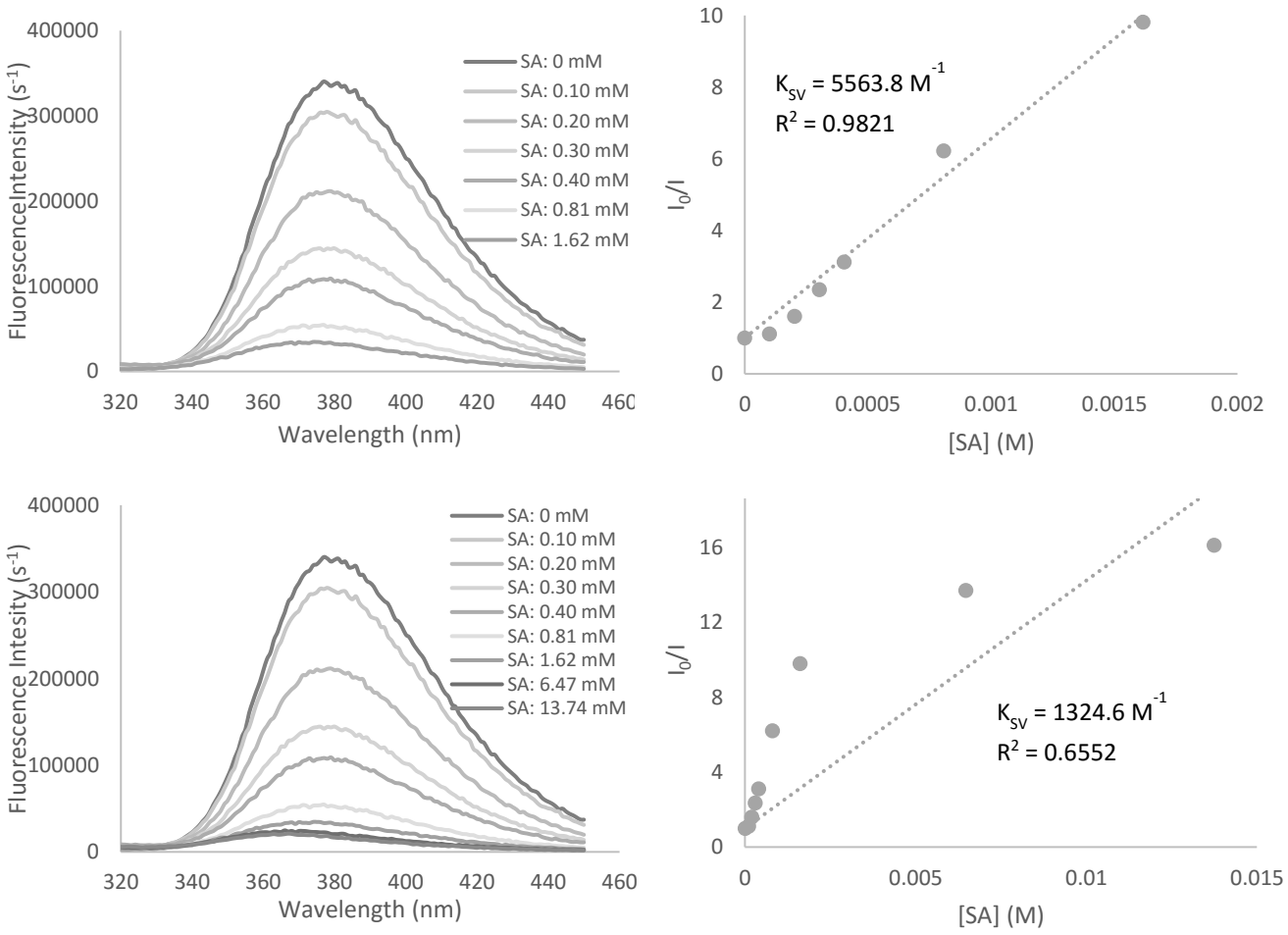

Figure 9. SA concentrations used past the saturation point skew results. Top left and right show the emission spectra and analysis of properly analysed MNP-SA binding, where R^2 value is close to 1. Bottom left and right show the same data with additional SA concentrations past the saturation point, where large increases in SA do not change the fluorescence much. This results in skewed K_{SV} data shown through the low R^2 value.

The emission spectra in the bottom left clearly shows very little difference in the fluorescence intensity of samples with SA concentrations above saturation point (in this case, 1.62 mM). These high concentrations cause a plateau to be formed in the analysis on the right, which renders linear regression inaccurate. The low R^2 value (shifting from 0.9821 previously to 0.6552) attests to this. Careful consideration must be taken to avoid using concentrations above the saturation point (which is usually noted qualitatively from the emission spectra and the graphical analysis, and quantitatively from the R^2 value), or else the reported data will be inaccurate (as in this case the Ksv changed from 5563.8 M^{-1} to 1324.6 M^{-1}).

3.3.5. **Correlating *in vitro* & *in vivo* mucoadhesion**

The results from the previous studies confirmed that PBA was indeed the mucoadhesive component of the MNPs, and that it was possible to quantify the binding between MNPs and SA. This prompted another query: as binding between MNPs and SA is the definition of mucoadhesion, was it possible to accurately predict the mucoadhesive capabilities of MNPs *in vivo* by doing *in vitro* tests? The *in vitro* tests were conducted to determine if they could detect small changes in mucoadhesion. MNPs with varying amounts of PBA functionalization (0, 10, 20, and 40 mg starting material) were nanoprecipitated and used for LSPR and fluorescence tests. The 10 mg starting material yielded 19.8 mol% PBA/dextran monomer, the 20 mg yielded 25.7 mol%, and the 40 mg yielded 46.2 mol%. The results are shown in Figure 10.

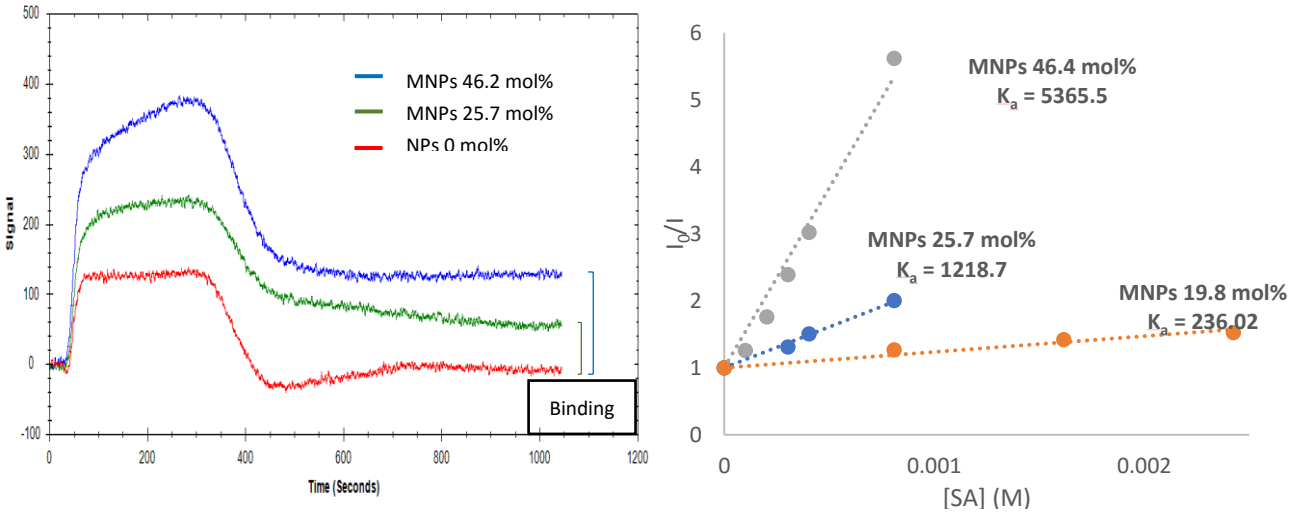

Figure 10. Utilizing in vitro studies to predict mucoadhesion of MNPs in vivo. LSPR graph (left) shows increased binding with increasing amounts of PBA. Analysis for K_A (right) shows increased K_A values for increasing PBA amounts.

LSPR showed overall an increased signal for increasing amounts of PBA in all stages of injection (the initial spike, the sustained injection period, and the end of the injection). Baseline stabilization post-injection of sample fell in line with the PBA values: 0 mg PBA had no increase in baseline, 20 mg PBA had a slight increase in baseline, and 40 mg PBA had the highest increase in baseline. This qualitatively shows real-time binding between the MNPs with different mol% of PBA to mucin on the AuNP surface, thus showing the LSPR's ability to detect different amounts of mucoadhesion.

This is followed up by quantitative studies with fluorescence in the graph on the right (conducted the same way as the previous studies). Linear regression revealed increasing K_A values for increasing amounts of PBA to start with when making the MNPs. The original MNP recipe yielded a K_A value of 5365.5 M^{-1}, the 25.7 mol% PBA gave 1218.7 M^{-1}, and the 19.8 mol% PBA gave 236.02 M^{-1}.

The two studies combined give a promising preview to what could be an innovative method to determine mucoadhesive capabilities *in vitro* without having to resort to *in vivo* methods. The

data presented here is still fairly preliminary, but the ability of the *in vitro* methods to be able to detect small changes in mucoadhesive capability could minimize animal studies in the future.

3.4. Conclusions

This chapter was dedicated to elucidating the binding kinetics between MNPs and SA in order to both better understand the binding model, and compare a binding constant value with literature values of SA-HA. LSPR opened a revealing window to the real-time binding which occurs between MNPs and mucin, and allowed a comparison with control PLA-Dex NPs and mucin. Using mucin was crucial to better mimic *in vivo* environments. It also allowed another confirmation of PBA as the mucoadhesive component in the MNPs. Fluorescence K_{SV} studies defined a facile quantitative measure of the binding between MNPs and SA, and the nature of binding between MNPs and SA allowed a more direct comparison with $K_{SV} = K_A$. The measured K_A of MNPs (5464.7 +/- 140.2 M^{-1}) was much higher than that reported in literature for SA-HA (333 – 500 M^{-1}). This affords a key advantage to MNPs in the quest to effectively treat influenza A, in that it is likely able to block binding between the influenza A virus to its target receptor SA.

Though the studies were initially designed as replacements for the hemagglutination inhibition assays conducted by many other publications, the *in vitro* tests became quite useful in their own right. After rigorous design regarding SA concentrations, coating parameters, etc. the result is a relatively facile set of tests. These were also expanded to being able to determine small differences in mucoadhesivity of the MNPs *in vitro*, and thus potentially remove the need for *in vivo* studies by predicting the capabilities themselves. This is preliminary work however.

The next step for the MNPs is to examine their properties after aerosolization, a process which will have to occur for their antiviral mechanism to take place (inhalation of MNPs). They are tested with CsA, a model drug.

Chapter 4. Characterizing aerosolized MNPs

4.1. MNP aerosolization and characterization

The next phase in determining MNPs' feasibility as an antiviral system was to determine their response to aerosolization. This is an important step, as their characteristics and morphology would ideally remain on par with their pre-aerosolized form, in order to retain their excellent ability for delivery and binding to mucosal membranes. The properties that were tested were morphology through TEM, drug encapsulation efficiency, drug weight loading, and drug release profiles through HPLC.

CsA is the active ingredient in Restasis®. Its hydrophobicity lends itself to being a good candidate for encapsulation by the MNPs in their hydrophobic PLA interior core. CsA also has uses in the respiratory tract, where it is used to treat idiopathic pulmonary fibrosis and improve lung function [113], [114]. This chapter uses CsA as the model drug to study how aerosolization affects the MNPs' ability to encapsulate and release drugs, though future studies will use more influenza-specific drugs such as oseltamivir.

4.2. Materials and methods

4.2.1. Materials

MNP formulation materials are the same as those is section 3.2.1. CsA was purchased from Sigma-Aldrich (Canada). TEM grids (F/C 400 mesh Cu) were purchased from Ted Pella (USA). Phosphotungstic acid was purchased from Fisher (Canada).

4.2.2. MNP preparation + drug encapsulation

Blank MNPs were prepared as described in section 3.2.2. The encapsulation of CsA in the MNPs was performed by nanoprecipitation. 1 mL of DMSO containing the PLA-Dex-PBA polymer (15 mg/mL) and CsA (varied concentration) was slowly added into 10 mL of Millipore

water under mild stirring for self-assembly of MNPs carrying the drugs. This was repeated once to ensure a final batch volume of 22 mL. The MNPs−CsA mixture was then syringe filtered (pore size = 200 nm) to remove NP or drug aggregates, and dialyzed against water to remove some of the free drugs and DMSO from the mixture.

4.2.3. **MNP characterization**

The sizes of the nanoparticles were determined using DLS, while the morphology of MNPs with no CsA (blank MNPs) was determined by TEM. Grids were prepared with 6.5 μL of sample and dried overnight, after which they were negatively stained with 20 mg/mL phosphotungstic acid.

The encapsulation efficiency and drug loading of CsA in the MNPs was determined using high-performance liquid chromatography (HPLC; C18 HPLC column, ACN/H2O 80:20 as the mobile phase with UV-absorption detection at 210 nm). 2 mL of the MNP-CsA solution was centrifuged in an Amicon Centrifugal Unit (MWCO = 10 kDa, Millipore Sigma) for 10 minutes at 8000 rpm to separate free CsA from the MNP-CsA compounds. The MNP-CsA compounds were then re-suspended in 10 mL acetonitrile before being run through HPLC. Labelling is as follows: MNPs-CsA-(wt%) where wt% is the drug weight% compared to the polymer. For example, MNPs-CsA-30% has 30 weight% of the polymer. Encapsulation efficiency was calculated as per Equation 2, where the actual concentration of drug measured in the sample is divided by the theoretical concentration of drug.

$$EE\% = \frac{[CsA]_{actual}}{[CsA]_{theoretical}} \times 100\%$$

Equation 2. Encapsulation efficiency

Drug loading was found by multiplying the encapsulation efficiency (not percentage) by the theoretical drug loading, as shown in Equation 3.

$$DL\% = EE \times DL\%_{theoretical}$$

Equation 3. Drug Loading

CsA's *in vitro* release profile from MNP-CsA was conducted through dialysis with DI as the release medium. 4 mL of sample was injected into a Slide-A-Lyzer dialysis cassette (MWCO: 20 kDa) and dialyzed against 120 mL of DI water at 37°C under mild stirring. 1 mL of the release medium was removed at each pre-determined time point (1, 3, 6, 12, 24, 48, 72, 96, and 120 h) to quantify the CsA release with HPLC, while 1 mL of fresh DI water was added to maintain a consistent volume.

4.2.4. **Aerosolization procedure**

Aerosolization of the MNPs was conducted with a Pari Nebulizer (LC® Sprint Reusable Nebulizer). MNPs or MNPs-CsA solution was added to the cup of the nebulizer post-dialysis to remove free drug and DMSO. The outlet was modified to suit the volume requirements of the experiment; while the nebulizer was designed for direct inhalation of the aerosols formed, the experiments required the samples to be in a liquid state for further characterization. To achieve this, the main exit point of the nebulizer was blocked off with parafilm, forcing the aerosols to climb to the top of the nebulizer where they were condensed back into liquid form and escaped into a centrifuge tube. 8 mL of MNPs-CsA yielded approximately 4-6 mL of aerosolized MNPs-CsA (MNPs-CsA-AER). All characterization methods were employed on both MNPs-CsA and MNPs-CsA-AER solutions.

4.3. Results & Discussion

4.3.1. TEM morphology characterization

The morphology of blank MNPs was examined pre- and post-aerosolization to determine if aerosolization had any adverse effects. Changes to morphology can skew encapsulation and release results. The TEM images are shown in Figure 11.

Pre-aerosolization

Post-aerosolization

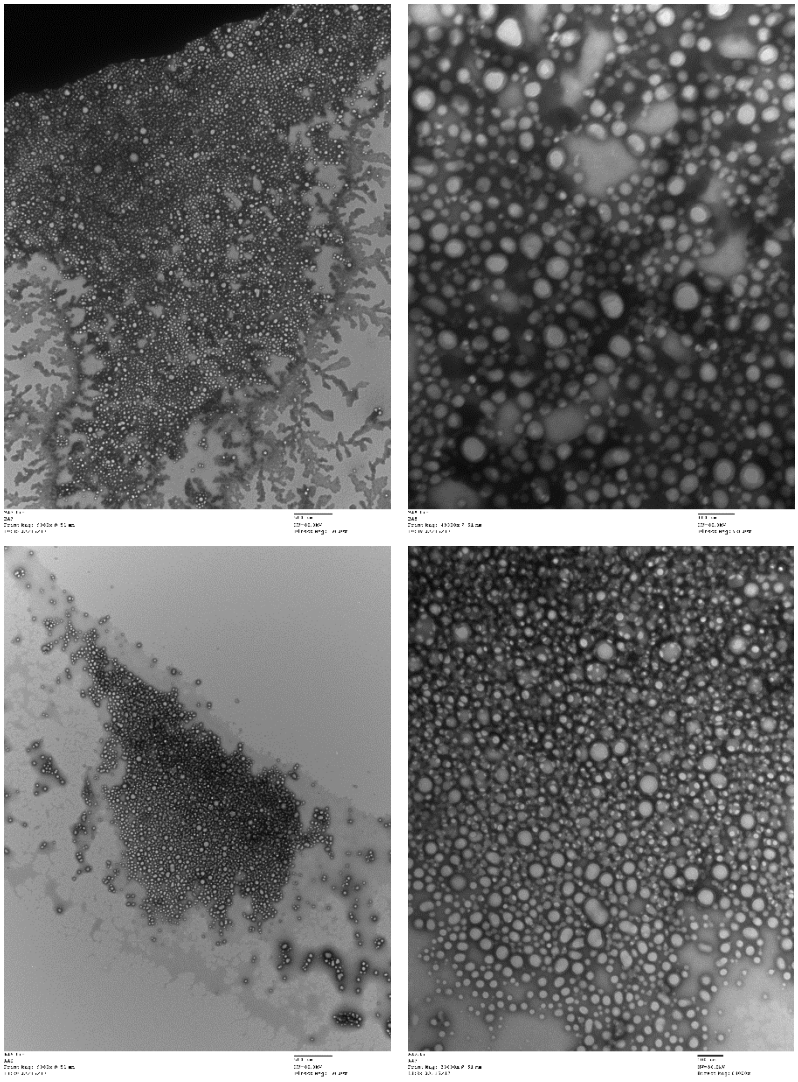

Figure 11. TEM images of blank MNPs pre and post-aerosolization. MNPs pre-aerosolization (top left: 500 nm scale bar, top right: 100 nm scale bar), MNPs post-aerosolization (bottom left: 500 nm scale bar, bottom right: 100 nm scale bar).

The zoomed out images on the left show similarities between pre- and post-aerosolization MNPs on a larger scale, with similar size spheres making up the grid. Once magnified, the images on the right show similar sizes and shapes, indicating the lack of adverse effects on morphology from aerosolization. This clears the path for blank MNPs' use in inhalation-based therapy; the next step determined how aerosolization affected their drug-encapsulating properties.

4.3.2. **DLS, encapsulation efficiency, and drug loading**

CsA was encapsulated in the MNPs at two weight percentages: 30 and 120%. The extremes of drug concentrations were explored to allow a better characterization of the MNPs' drug loading abilities. The samples were measured by DLS for their size and polydispersity (PDI), and HPLC for their encapsulation efficiency (EE) and drug loading (DL). Results are shown in Table 2.

Table 2. Characterization of MNPs-CsA and MNPs-CsA-AER

	DLS (nm)	**PDI**	**EE (%)**	**DL (%)**
Blank MNPs	50.6	0.085	-	-
MNPs-CsA-30%	69.1	0.063	77.54	23.36
MNPs-CsA-30%-AER	287.7	0.359	62.62	18.79
MNPs-CsA-120%	135.4	0.088	84.28	101.14
MNPs-CsA-120%-AER	517.9	0.167	84.29	101.15

DLS results showed increasing size with increasing drug concentration in both MNPs-CsA and MNPs-CsA-AER. The sizes increased somewhat after aerosolization, possibly due to aggregation from the condensation of the aerosols. Though not ideal, it is not a cause of worry as the encapsulation efficiencies and drug loading are relatively unaffected by aerosolization. Both the 30 and 120 wt% showed high encapsulation efficiencies, and aerosolization seemed to keep

them relatively stable (more so for the higher wt%, likely due to the larger amount of drug available in the solution). Indeed, the 120% had no real change in encapsulation efficiency, staying at 84%. The drug loading calculation shows the actual drug/polymer ratio which was loaded in the MNPs, and so is ideally 30 or 120%. The results show very high drug loading for both MNPs-CsA samples, very close to the theoretical drug loading. The results were again virtually unchanged post-aerosolization, highlighting the lack of negative effects from aerosolization on the MNPs.

4.3.3. **Release study**

Finally, the release profile of MNPs-CsA pre- and post-aerosolization was evaluated. DI water was used as the release medium as used in other such studies [115]. The profiles of all four samples are show in in Figure 12.

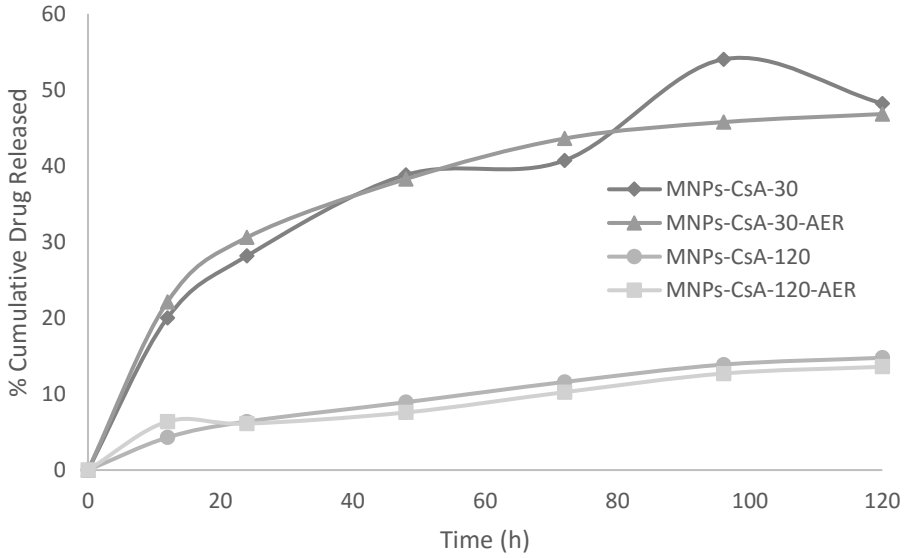

Figure 12. Release profile of MNPs-CsA and MNPs-CsA-AER at two different wt% (30 and 120%). Measurements were taken over a 5 day period.

As can be seen, the 30 wt% samples generally released more than their 120 wt% counterparts. This may be due to the increased amount of hydrophobic drug in the 120 wt% sample being more bound-up in the core due to hydrophobic interactions than with the lower

concentration, thus releasing less of the cumulative drug amount. Both concentrations show an initial burst release (to different degrees) and then steady, sustained release over the measured time points. Focusing on simply pre- and post-aerosolized MNPs shows remarkably similar trends in release profiles. Aerosolization seems to have little effect on the MNPs' ability to release encapsulated drugs.

4.4. Conclusions

This chapter examined the effect of aerosolization on blank MNPs and MNPs carrying a model drug (CsA). The ability to withstand aerosolization is an important parameter for MNPs as their intended target, influenza in the lungs, will be best reached by inhalation (the same manner in which influenza infection occurs).

Blank MNPs responded well to aerosolization with no real morphological changes as seen by TEM. Though DLS on CsA-encapsulated MNPs showed an increase in diameter, the size changes did not affect the MNPs' abilities to encapsulate and release CsA. Encapsulation efficiencies and drug loading were quite high in both CsA weight percents which were tested, and the release profile into DI was quite steady and similar between pre- and post-aerosolized samples.

CsA was used as a model drug due to its use in aiding pulmonary function, its hydrophobic nature, and its ability to be encapsulated in MNPs as examined previously for ocular delivery. As this model drug is not affected by the aerosolization procedure, the next step to this study will be to repeat such tests with a drug more relevant to treatment of influenza A such as oseltamivir.

Chapter 5. Conclusions & Future Work

5.1. Conclusions

The goal of this thesis work was to examine the possibility of using mucoadhesive nanoparticles as antiviral therapeutics for the influenza A virus. Its similar mechanism of use in ocular drug delivery lent itself to exploration in pulmonary delivery. To that end, a thorough literature review was conducted to determine the current uses of nanoparticles in influenza A treatment. Based off this, it was decided to go forward with testing MNPs as polymeric NPs had not been fully explored in their capacity as antiviral therapeutics.

The MNPs were first tested for their ability to bind to the mucus membrane (and sialic acid specifically) through localized surface plasmon resonance and fluorescence studies. These experiments cemented the MNPs' mechanism of mucoadhesion (PBA binding covalently to sialic acid) and resulted in qualitative and quantitative binding kinetic data for the MNPs through the Stern-Volmer equation. The K_A value for MNPs with sialic acid was determined to be 5464.7 +/- 140.2 M^{-1}, which is far higher than the literature values of 333-500 M^{-1} for sialic acid-hemagglutinin. This gave confidence to the initial hypothesis of MNPs' candidacy for antiviral therapeutics. During these experiments, another use for binding kinetics studies was discovered: the potential to predict mucoadhesion from LSPR and fluorescence *in vitro* as opposed to conducting *in vivo* work. The methods were able detect differences in binding constants and general binding in MNPs with different amounts of PBA attached, a first-step in this process.

The next step in determining the MNPs' viability for antiviral therapeutics was to check for changes in key properties and characteristics after aerosolization. Aerosolization is a major component for effective antiviral treatment, and morphology, drug encapsulation properties, and release profiles of the MNPs were tested and compared for pre- and post-aerosolization MNPs.

CsA was used as a model drug due to its previous encapsulation in MNPs and its use in aiding pulmonary function. Morphology remained similar for blank MNPs pre- and post-aerosolization, and though sizes did increase, encapsulation efficiencies, drug loading, and release profiles did not differ significantly for MNPs encapsulating CsA.

5.2. Future Work

The research objectives outlined in section 1.2 were met through this body of work, and paved the way for future studies.

The next step for assessing MNPs' viability as antiviral therapeutics will be to load antiviral drugs and observe their properties. Oseltamivir, due to its hydrophobic nature, would be an excellent candidate to attempt encapsulation. Once encapsulation has been achieved, drug release propertied should be determined. Using oseltamivir in this way allows a multivalent approach to fighting influenza, where MNPs act as both a drug-carrier and an inhibitor themselves.

An *in vitro* study is recommended to properly assess the antiviral capabilities of MNPs with oseltamivir against live virus. Many examples of these are shown in Chapter 2, where MDCK cells are infected with live virus strains and treated with the antiviral compound. A suggestion to improve the typical study would be to layer the MDCK cells with mucin to more properly mimic *in vivo* conditions.

Simulations could be used to model the binding between MNPs and sialic acid, and compare it to hemagglutinin and sialic acid. This would impart a greater understanding of the bond, and provide methods of improvement.

The preliminary data from the correlating *in vitro* and *in vivo* mucoadhesion study shows promise in predicting mucoadhesive capabilities. This study should be furthered with more

replicates of the current data, and finally *in vivo* studies to corroborate the differences detected by the *in vitro* method.

Finally, an *in vivo* study should be conducted for aerosolized MNPs to determine their bioavailability in the lungs. Theoretically, MNPs should be able to settle well into the pulmonary tract due to their nanoscale size. Their mucoadhesive function should also afford some protection from rapid clearance. An in-depth murine *in vivo* study would confirm these hypotheses, and conclusively reveal which diseases would be ideal for use of MNPs in treatment.

References

[1] Y. Zhang et al.., “Development and evaluation of mucoadhesive nanoparticles based on thiolated Eudragit for oral delivery of protein drugs,” *J. Nanoparticle Res.*, vol. 17, no. 2, p. 98, Feb. 2015.

[2] U. Bhosale, D. V Kusum, and N. Jain, “Formulation and optimization of mucoadhesive nanodrug delivery system of acyclovir.,” *J. Young Pharm.*, vol. 3, no. 4, pp. 275–83, Oct. 2011.

[3] H. K. Ibrahim, I. S. El-Leithy, and A. A. Makky, “Mucoadhesive Nanoparticles as Carrier Systems for Prolonged Ocular Delivery of Gatifloxacin/Prednisolone Bitherapy,” *Mol. Pharm.*, vol. 7, no. 2, pp. 576–585, Apr. 2010.

[4] S. Liu et al.., “Prolonged Ocular Retention of Mucoadhesive Nanoparticle Eye Drop Formulation Enables Treatment of Eye Diseases Using Significantly Reduced Dosage,” *Mol. Pharm.*, vol. 13, no. 9, pp. 2897–2905, Sep. 2016.

[5] Y. Suzuki et al.., “Sialic acid species as a determinant of the host range of influenza A viruses.,” *J. Virol.*, vol. 74, no. 24, pp. 11825–31, Dec. 2000.

[6] J. H. Draize, G. Woodard, and H. O. Calvery, “METHODS FOR THE STUDY OF IRRITATION AND TOXICITY OF SUBSTANCES APPLIED TOPICALLY TO THE SKIN AND MUCOUS MEMBRANES,” *J. Pharmacol. Exp. Ther.*, pp. 377–390, 1944.

[7] “WHO | Influenza (Seasonal),” *WHO*, 2016. [Online]. Available: http://www.who.int/mediacentre/factsheets/fs211/en/. [Accessed: 24-Jul-2017].

[8] C. Gerdil, “The annual production cycle for influenza vaccine,” *Vaccine*, vol. 21, no. 16, pp. 1776–1779, May 2003.

[9] G. A. Poland, R. M. Jacobson, and I. G. Ovsyannikova, “Influenza virus resistance to antiviral agents: a plea for rational use.,” *Clin. Infect. Dis.*, vol. 48, no. 9, pp. 1254–6, May 2009.

[10] E. Goldstein and M. Lipsitch, “Antiviral usage for H1N1 treatment: pros, cons and an argument for broader prescribing guidelines in the United States.,” *PLoS Curr.*, vol. 1, p. RRN1122, Oct. 2009.

[11] J. B. Mahony, S. Chong, K. Luinstra, A. Petrich, and M. Smieja, “Development of a novel bead-

based multiplex PCR assay for combined subtyping and oseltamivir resistance genotyping (H275Y) of seasonal and pandemic H1N1 influenza A viruses," *J. Clin. Virol.*, vol. 49, no. 4, pp. 277–282, Dec. 2010.

[12] J. Wilschut, J. E. McElhaney, and A. M. Palache, *Influenza*, 2nd ed. Edinburgh: Mosby Elsevier, 2006.

[13] E. Nobusawa and K. Sato, "Comparison of the mutation rates of human influenza A and B viruses.," *J. Virol.*, vol. 80, no. 7, pp. 3675–8, Apr. 2006.

[14] R. A. Lamb and P. W. Choppin, "The Gene Structure and Replication of Influenza Virus," *Annu. Rev. Biochem.*, vol. 52, no. 1, pp. 467–506, Jun. 1983.

[15] N. M. Bouvier and P. Palese, "The biology of influenza viruses.," *Vaccine*, vol. 26, no. Suppl 4, pp. D49-53, Sep. 2008.

[16] S. L. Zebedee and R. A. Lamb, "Influenza A virus M2 protein: monoclonal antibody restriction of virus growth and detection of M2 in virions.," *J. Virol.*, vol. 62, no. 8, pp. 2762–72, Aug. 1988.

[17] "A revision of the system of nomenclature for influenza viruses: a WHO memorandum.," *Bull. World Health Organ.*, vol. 58, no. 4, pp. 585–91, 1980.

[18] T. Samji, "Influenza A: understanding the viral life cycle.," *Yale J. Biol. Med.*, vol. 82, no. 4, pp. 153–9, Dec. 2009.

[19] I. A. Wilson, J. J. Skehel, and D. C. Wiley, "Structure of the haemagglutinin membrane glycoprotein of influenza virus at 3 A resolution.," *Nature*, vol. 289, no. 5796, pp. 366–73, Jan. 1981.

[20] P. M. Colman, J. N. Varghese, and W. G. Laver, "Structure of the catalytic and antigenic sites in influenza virus neuraminidase.," *Nature*, vol. 303, no. 5912, pp. 41–4.

[21] L. J. Holsinger and R. A. Lamb, "Influenza virus M2 integral membrane protein is a homotetramer stabilized by formation of disulfide bonds.," *Virology*, vol. 183, no. 1, pp. 32–43, Jul. 1991.

[22] E. Ghedin et al.., "Large-scale sequencing of human influenza reveals the dynamic nature of viral genome evolution," *Nature*, vol. 437, no. 7062, pp. 1162–1166, Oct. 2005.

[23] C. B. Hall and C. B. Hall, "The Spread of Influenza and Other Respiratory Viruses: Complexities

and Conjectures," *Clin. Infect. Dis.*, vol. 45, pp. 353–9, 2007.

[24] J. E. Stencel-Baerenwald, K. Reiss, D. M. Reiter, T. Stehle, and T. S. Dermody, "Viral attachment to receptors that are expressed on host cells initiates infection and therefore, viral receptors are determinants of host range and govern host cell suscep- tibility. Various cell surface carbohydrates, including sialylated glycans," *Nat. Publ. Gr.*, vol. 12, 2014.

[25] A.-K. Sauer et al.., "Characterization of the Sialic Acid Binding Activity of Influenza A Viruses Using Soluble Variants of the H7 and H9 Hemagglutinins," *PLoS One*, vol. 9, no. 2, p. e89529, Feb. 2014.

[26] S. J. Gamblin and J. J. Skehel, "Influenza hemagglutinin and neuraminidase membrane glycoproteins.," *J. Biol. Chem.*, vol. 285, no. 37, pp. 28403–9, Sep. 2010.

[27] D. A. Steinhauer, "Role of Hemagglutinin Cleavage for the Pathogenicity of Influenza Virus," *Virology*, vol. 258, no. 1, pp. 1–20, May 1999.

[28] S. B. Sieczkarski and G. R. Whittaker, "Viral entry.," *Curr. Top. Microbiol. Immunol.*, vol. 285, pp. 1–23, 2005.

[29] T. Stegmann, "Membrane fusion mechanisms: the influenza hemagglutinin paradigm and its implications for intracellular fusion.," *Traffic*, vol. 1, no. 8, pp. 598–604, Aug. 2000.

[30] K. Martin and A. Helenius, "Transport of incoming influenza virus nucleocapsids into the nucleus.," *J. Virol.*, vol. 65, no. 1, pp. 232–44, Jan. 1991.

[31] J. F. Cros and P. Palese, "Trafficking of viral genomic RNA into and out of the nucleus: influenza, Thogoto and Borna disease viruses.," *Virus Res.*, vol. 95, no. 1–2, pp. 3–12, Sep. 2003.

[32] R. M. Krug, "Priming of influenza viral RNA transcription by capped heterologous RNAs.," *Curr. Top. Microbiol. Immunol.*, vol. 93, pp. 125–49, 1981.

[33] C. T. Bancroft and T. G. Parslow, "Evidence for segment-nonspecific packaging of the influenza a virus genome.," *J. Virol.*, vol. 76, no. 14, pp. 7133–9, Jul. 2002.

[34] Y. Fujii, H. Goto, T. Watanabe, T. Yoshida, and Y. Kawaoka, "Selective incorporation of influenza virus RNA segments into virions," *Proc. Natl. Acad. Sci.*, vol. 100, no. 4, pp. 2002–2007, Feb. 2003.

[35] L. M. Burleigh, L. J. Calder, J. J. Skehel, and D. A. Steinhauer, “Influenza A Viruses with Mutations in the M1 Helix Six Domain Display a Wide Variety of Morphological Phenotypes,” *J. Virol.*, vol. 79, no. 2, pp. 1262–1270, Jan. 2005.

[36] P. Palese, K. Tobita, M. Ueda, and R. W. Compans, “Characterization of temperature sensitive influenza virus mutants defective in neuraminidase.,” *Virology*, vol. 61, no. 2, pp. 397–410, Oct. 1974.

[37] P. C. Soema, R. Kompier, J.-P. Amorij, and G. F. A. Kersten, “Current and next generation influenza vaccines: Formulation and production strategies,” *Eur. J. Pharm. Biopharm.*, vol. 94, pp. 251–263, Aug. 2015.

[38] A. Moscona, “Neuraminidase Inhibitors for Influenza,” *N. Engl. J. Med.*, vol. 353, no. 13, pp. 1363–1373, Sep. 2005.

[39] R. A. Bright et al.., “Incidence of adamantane resistance among influenza A (H3N2) viruses isolated worldwide from 1994 to 2005: a cause for concern,” *Lancet*, vol. 366, no. 9492, pp. 1175–1181, Oct. 2005.

[40] L. V Gubareva, L. Kaiser, and F. G. Hayden, “Influenza virus neuraminidase inhibitors,” *Lancet*, vol. 355, no. 9206, pp. 827–835, Mar. 2000.

[41] T. G. Sheu et al.., “Surveillance for Neuraminidase Inhibitor Resistance among Human Influenza A and B Viruses Circulating Worldwide from 2004 to 2008,” *Antimicrob. Agents Chemother.*, vol. 52, no. 9, pp. 3284–3292, Sep. 2008.

[42] I. Stephenson et al.., “Neuraminidase Inhibitor Resistance after Oseltamivir Treatment of Acute Influenza A and B in Children,” *Clin. Infect. Dis.*, vol. 48, no. 4, pp. 389–396, Feb. 2009.

[43] V. Escuret et al.., “Detection of human influenza A (H1N1) and B strains with reduced sensitivity to neuraminidase inhibitors,” *J. Clin. Virol.*, vol. 41, no. 1, pp. 25–28, Jan. 2008.

[44] R. Dolin, R. C. Reichman, H. P. Madore, R. Maynard, P. N. Linton, and J. Webber-Jones, “A Controlled Trial of Amantadine and Rimantadine in the Prophylaxis of Influenza a Infection,” *N. Engl. J. Med.*, vol. 307, no. 10, pp. 580–584, Sep. 1982.

[45] R. B. Belshe, M. H. Smith, C. B. Hall, R. Betts, and A. J. Hay, “Genetic basis of resistance to rimantadine emerging during treatment of influenza virus infection.,” *J. Virol.*, vol. 62, no. 5, pp. 1508–12, May 1988.

[46] R. A. Bright, D. K. Shay, B. Shu, N. J. Cox, and A. I. Klimov, “Adamantane Resistance Among Influenza A Viruses Isolated Early During the 2005-2006 Influenza Season in the United States,” *JAMA*, vol. 295, no. 8, p. 891, Feb. 2006.

[47] G. A. Poland, R. M. Jacobson, and I. G. Ovsyannikova, “Influenza virus resistance to antiviral agents: a plea for rational use.,” *Clin. Infect. Dis.*, vol. 48, no. 9, pp. 1254–6, May 2009.

[48] S. Galdiero, A. Falanga, M. Vitiello, M. Cantisani, V. Marra, and M. Galdiero, “Silver Nanoparticles as Potential Antiviral Agents,” *Molecules*, vol. 16, no. 12, pp. 8894–8918, Oct. 2011.

[49] W. H. De Jong and P. J. A. Borm, “Drug delivery and nanoparticles:applications and hazards.,” *Int. J. Nanomedicine*, vol. 3, no. 2, pp. 133–49, 2008.

[50] O. R. Miranda et al.., “Colorimetric Bacteria Sensing Using a Supramolecular Enzyme–Nanoparticle Biosensor,” *J. Am. Chem. Soc.*, vol. 133, no. 25, pp. 9650–9653, Jun. 2011.

[51] C. E. Probst, P. Zrazhevskiy, V. Bagalkot, and X. Gao, “Quantum dots as a platform for nanoparticle drug delivery vehicle design,” *Adv. Drug Deliv. Rev.*, vol. 65, no. 5, pp. 703–718, May 2013.

[52] F. Danhier, E. Ansorena, J. M. Silva, R. Coco, A. Le Breton, and V. Préat, “PLGA-based nanoparticles: An overview of biomedical applications,” *J. Control. Release*, vol. 161, no. 2, pp. 505–522, Jul. 2012.

[53] J.-L. Gong et al.., “Ag/SiO2 core-shell nanoparticle-based surface-enhanced Raman probes for immunoassay of cancer marker using silica-coated magnetic nanoparticles as separation tools,” *Biosens. Bioelectron.*, vol. 22, no. 7, pp. 1501–1507, Feb. 2007.

[54] L. Dykman and N. Khlebtsov, “Gold nanoparticles in biomedical applications: recent advances and perspectives,” *Chem. Soc. Rev.*, vol. 41, no. 6, pp. 2256–2282, Feb. 2012.

[55] L. C. Kennedy et al.., “A New Era for Cancer Treatment: Gold-Nanoparticle-Mediated Thermal Therapies,” *Small*, vol. 7, no. 2, pp. 169–183, Jan. 2011.

[56] M. Geiser and W. Kreyling, “Deposition and biokinetics of inhaled nanoparticles,” *Part. Fibre Toxicol.*, vol. 7, no. 2, Jan. 2010.

[57] B. S. Bender and P. A. Small, “Influenza: pathogenesis and host defense.,” *Semin. Respir. Infect.*, vol. 7, no. 1, pp. 38–45, Mar. 1992.

[58] D.-X. Xiang, Q. Chen, L. Pang, and C.-L. Zheng, “Inhibitory effects of silver nanoparticles on H1N1 influenza A virus *in vitro*,” *J. Virol. Methods*, vol. 178, pp. 137–142, 2011.

[59] M. Fatima, N. us S. S. Zaidi, D. Amraiz, and F. Afzal, “*In vitro* antiviral activity of Cinnamomum cassia and its nanoparticles against H7N3 influenza a virus,” *J. Microbiol. Biotechnol.*, vol. 26, no. 1, pp. 151–159, 2016.

[60] P. Mehrbod et al.., “*In vitro* Antiviral Effect of ‘Nanosilver’ on Influenza Virus,” *DARU J. Pharm. Sci.*, vol. 17, no. 2, pp. 88–93, 2009.

[61] D. Xiang et al.., “Inhibition of A/Human/Hubei/3/2005 (H3N2) influenza virus infection by silver nanoparticles *in vitro* and *in vivo*.,” *Int. J. Nanomedicine*, vol. 8, pp. 4103–13, 2013.

[62] Z. Lin et al.., “The inhibition of H1N1 influenza virus-induced apoptosis by silver nanoparticles functionalized with zanamivir,” *RSC Adv.*, vol. 7, pp. 742–740, 2017.

[63] Y. Li et al.., “Silver Nanoparticle Based Codelivery of Oseltamivir to Inhibit the Activity of the H1N1 Influenza Virus through ROS-Mediated Signaling Pathways,” *Appl. Mater. Interfaces*, vol. 8, pp. 24385–24393, 2016.

[64] Y. Li et al.., “Reversal of H1N1 influenza virus-induced apoptosis by silver nanoparticles functionalized with amantadine,” *RSC Adv.*, vol. 6, no. 92, pp. 89679–89686, 2016.

[65] Z. Zhang et al.., “Influenza-binding sialylated polymer coated gold nanoparticles prepared via RAFT polymerization and reductive amination,” *Chem. Commun. Chem. Commun*, vol. 3352, no. 52, pp. 3352–3355, 2016.

[66] Fei Feng1 et al.., “Novel thiosialosides tethered to metal nanoparticles as potent influenza A virus haemagglutinin blockers,” *Antivir. Chem. Chemother.*, vol. 23, pp. 59–65, 2013.

[67] I. Papp et al.., “Inhibition of influenza virus infection by multivalent sialic-acid-functionalized gold

nanoparticles.," *Small*, vol. 6, no. 24, pp. 2900–2906, 2010.

[68] M. Stanley et al.., "'TamiGold': phospha-oseltamivir-stabilised gold nanoparticles as the basis for influenza therapeutics and diagnostics targeting the neuraminidase (instead of the hemagglutinin)," *Medchemcomm*, vol. 3, no. 11, p. 1373, Oct. 2012.

[69] N. V. S. N. A. Mazurkovaa, Yu. E. Spitsynaa, Z. R. Ismagilovc, S. N. Zagrebel'nyia, and and E. I. Ryabchikovaa, "Interaction of Titanium Dioxide Nanoparticles with Influenza Virus," *Nanotechnologies Russ.*, vol. 5, pp. 417–420, 2010.

[70] M. Repkova et al.., "Efficient inhibition of influenza A viral replication in cells by deoxyribozymes delivered by nanocomposites," *Int. J. Antimicrob. Agents*, vol. 49, pp. 703–708, 2017.

[71] J.-J. Liang, J.-C. Wei, Y.-L. Lee, S. Hsu, J.-J. Lin, and Y.-L. Lin, "Surfactant-modified nanoclay exhibits an antiviral activity with high potency and broad spectrum.," *J. Virol.*, vol. 88, no. 8, pp. 4218–28, Apr. 2014.

[72] R. Kumar et al.., "Antiviral effect of Glycine coated Iron oxide nanoparticles iron against H1N1 influenza A virus," *Int. J. Infect. Dis.*, vol. 45, pp. 281–282, Apr. 2016.

[73] S.-J. Kwon et al.., "Nanostructured glycan architecture is important in the inhibition of influenza A virus infection," *Nat. Nanotechnol.*, vol. 12, pp. 48–56, 2017.

[74] S. Bhatia et al.., "Linear polysialoside outperforms dendritic analogs for inhibition of influenza virus infection *in vitro* and *in vivo*," *Biomaterials*, vol. 138, pp. 22–34, 2017.

[75] A. Nazemi, S. M. M. Haeryfar, and E. R. Gillies, "Multifunctional Dendritic Sialopolymersomes as Potential Antiviral Agents: Their Lectin Binding and Drug Release Properties," *Langmuir*, vol. 29, pp. 6420–6428, 2013.

[76] M. Ogata et al.., "Synthesis of multivalent sialyllactosamine-carrying glyco-nanoparticles with high affinity to the human influenza virus hemagglutinin," *Carbohydr. Polym.*, vol. 153, pp. 96–104, 2016.

[77] J. S. Kim et al.., "Antimicrobial effects of silver nanoparticles," *Nanomedicine Nanotechnology, Biol. Med.*, vol. 3, no. 1, pp. 95–101, Mar. 2007.

[78] M. Rai, A. Yadav, and A. Gade, “Silver nanoparticles as a new generation of antimicrobials,” *Biotechnol. Adv.*, vol. 27, no. 1, pp. 76–83, Jan. 2009.

[79] J. H. Miller et al.., “Effect of silver nanoparticles and antibiotics on antibiotic resistance genes in anaerobic digestion.,” *Water Environ. Res.*, vol. 85, no. 5, pp. 411–21, May 2013.

[80] V. Kumar and S. K. Yadav, “Plant-mediated synthesis of silver and gold nanoparticles and their applications,” *J. Chem. Technol. Biotechnol.*, vol. 84, no. 2, pp. 151–157, Feb. 2009.

[81] Y. Sun and Y. Xia, “Shape-Controlled Synthesis of Gold and Silver Nanoparticles,” *Science (80-.).*, vol. 298, no. 5601, 2002.

[82] R. Levi, T. Beeor-Tzahar, and R. Arnon, “Microculture virus titration — a simple colourimetric assay for influenza virus titration,” *J. Virol. Methods*, vol. 52, no. 1–2, pp. 55–64, Mar. 1995.

[83] D.-X. Xiang, Q. Chen, L. Pang, and C.-L. Zheng, “Inhibitory effects of silver nanoparticles on H1N1 influenza A virus *in vitro*,” *J. Virol. Methods*, vol. 178, pp. 137–142, 2011.

[84] M.-C. Daniel and D. Astruc, “Gold Nanoparticles: Assembly, Supramolecular Chemistry, Quantum-Size-Related Properties, and Applications toward Biology, Catalysis, and Nanotechnology,” *Chem. Rev.*, vol. 104, pp. 293–346, 2004.

[85] E. E. Connor, J. Mwamuka, A. Gole, C. J. Murphy, and M. D. Wyatt, “Gold Nanoparticles Are Taken Up by Human Cells but Do Not Cause Acute Cytotoxicity,” *Small*, vol. 1, no. 3, pp. 325–327, Mar. 2005.

[86] P. GHOSH, G. HAN, M. DE, C. KIM, and V. ROTELLO, “Gold nanoparticles in delivery applications,” *Adv. Drug Deliv. Rev.*, vol. 60, no. 11, pp. 1307–1315, Aug. 2008.

[87] A. M. Paul et al.., “Delivery of antiviral small interfering RNA with gold nanoparticles inhibits dengue virus infection *in vitro*,” *J. Gen. Virol.*, vol. 95, no. Pt_8, pp. 1712–1722, Aug. 2014.

[88] C. Garrido et al.., “Gold nanoparticles to improve HIV drug delivery.,” *Future Med. Chem.*, vol. 7, no. 9, pp. 1097–107, 2015.

[89] C. E. Peña-González et al.., “Dendronized Anionic Gold Nanoparticles: Synthesis, Characterization, and Antiviral Activity,” *Chem. - A Eur. J.*, vol. 22, no. 9, pp. 2987–2999, Feb. 2016.

[90] Tobias J. Brunner et al.., "*In vitro* Cytotoxicity of Oxide Nanoparticles: Comparison to Asbestos, Silica, and the Effect of Particle Solubility," *Environ. Sci. Technol.*, vol. 40, no. 14, pp. 4374–4381, 2006.

[91] Y. Kubota et al.., "Photokilling of T-24 human bladder cancer cells with titanium dioxide.," *Br. J. Cancer*, vol. 70, no. 6, pp. 1107–11, Dec. 1994.

[92] D. Guo, C. Wu, H. Jiang, Q. Li, X. Wang, and B. Chen, "Synergistic cytotoxic effect of different sized ZnO nanoparticles and daunorubicin against leukemia cancer cells under UV irradiation," *J. Photochem. Photobiol. B Biol.*, vol. 93, no. 3, pp. 119–126, Dec. 2008.

[93] C. A. Hong and Y. S. Nam, "Functional Nanostructures for Effective Delivery of Small Interfering RNA Therapeutics," *Theranostics*, vol. 4, no. 12, pp. 1211–1232, 2014.

[94] K. S. Soppimath, T. M. Aminabhavi, A. R. Kulkarni, and W. E. Rudzinski, "Biodegradable polymeric nanoparticles as drug delivery devices," *J. Control. Release*, vol. 70, no. 1–2, pp. 1–20, Jan. 2001.

[95] A. Kumari, S. K. Yadav, and S. C. Yadav, "Biodegradable polymeric nanoparticles based drug delivery systems," *Colloids Surfaces B Biointerfaces*, vol. 75, no. 1, pp. 1–18, Jan. 2010.

[96] J. M. Chan, P. M. Valencia, L. Zhang, R. Langer, and O. C. Farokhzad, "Polymeric Nanoparticles for Drug Delivery," in *Methods in molecular biology (Clifton, N.J.)*, vol. 624, 2010, pp. 163–175.

[97] A.-M. Caminade et al.., "Dendrimers for drug delivery," *J. Mater. Chem. B*, vol. 2, no. 26, pp. 4055–4066, 2014.

[98] R. Esfand and D. A. Tomalia, "Poly(amidoamine) (PAMAM) dendrimers: from biomimicry to drug delivery and biomedical applications," *Drug Discov. Today*, vol. 6, no. 8, pp. 427–436, Apr. 2001.

[99] Y. Takemoto et al.., "Synthesis of highly branched anionic α-glucans by thermostable phosphorylase-catalyzed α-glucuronylation," *Carbohydr. Res.*, vol. 366, pp. 38–44, Jan. 2013.

[100] N. G. N. Swamy and Z. Abbas, "Preparation and *in vitro* characterization of mucoadhesive hydroxypropyl guar microspheres containing amlodipine besylate for nasal administration.," *Indian J. Pharm. Sci.*, vol. 73, no. 6, pp. 608–14, Nov. 2011.

[101] R. B. Ramesha Chary, G. Vani, and Y. M. Rao, "*In vitro* and *In vivo* Adhesion Testing of Mucoadhesive Drug Delivery Systems," *Drug Dev. Ind. Pharm.*, vol. 25, no. 5, pp. 685–690, Jan. 1999.

[102] S. T. Lim, G. P. Martin, D. J. Berry, and M. B. Brown, "Preparation and evaluation of the *in vitro* drug release properties and mucoadhesion of novel microspheres of hyaluronic acid and chitosan.," *J. Control. Release*, vol. 66, no. 2–3, pp. 281–92, May 2000.

[103] G. Springsteen and B. Wang, "A detailed examination of boronic acid-diol complexation," *Tetrahedron*, vol. 58, pp. 5291–5300, 2002.

[104] N. K. Sauter et al.., "Hemagglutinins from two influenza virus variants bind to sialic acid derivatives with millimolar dissociation constants: A 500-MHz Proton nuclear magnetic resonance study," *Biochemistry*, vol. 28, no. 21. pp. 8388–8396, 1989.

[105] W. Weis, J. H. Brown, S. Cusack, J. C. Paulson, J. J. Skehel, and D. C. Wiley, "Structure of the influenza virus haemagglutinin complexed with its receptor, sialic acid.," *Nature*, vol. 333, no. 6172, pp. 426–431, 1988.

[106] S. Liu, L. Jones, and F. X. Gu, "Development of Mucoadhesive Drug Delivery System Using Phenylboronic Acid Functionalized Poly(D , L -lactide)- *b* -Dextran Nanoparticles," *Macromol. Biosci.*, vol. 12, no. 12, pp. 1622–1626, Dec. 2012.

[107] J. Mitchell, "Small Molecule Immunosensing Using Surface Plasmon Resonance," *Sensors*, vol. 10, no. 8, pp. 7323–7346, Aug. 2010.

[108] S. Deshayes et al.., "Phenylboronic Acid-Installed Polymeric Micelles for Targeting Sialylated Epitopes in Solid Tumors," *J. Am. Chem. Soc.*, vol. 135, no. 41, pp. 15501–15507, Oct. 2013.

[109] K. Djanashvili, L. Frullano, and J. A. Peters, "Molecular Recognition of Sialic Acid End Groups by Phenylboronates," *Chemistry (Easton).*, vol. 11, no. 13, pp. 4010–4018, Jun. 2005.

[110] H. Otsuka, E. Uchimura, H. Koshino, T. Okano, and K. Kataoka, "Anomalous Binding Profile of Phenylboronic Acid with N-Acetylneuraminic Acid (Neu5Ac) in Aqueous Solution with Varying pH," *JACS*, vol. 125, no. 12, pp. 3493–3502, 2003.

[111] K. Kur-Kowalska, M. Przybyt, P. Ziółczyk, P. Sowiński, and E. Miller, “Fluorescence properties of 3-amino phenylboronic acid and its interaction with glucose and ZnS:Cu quantum dots,” *Spectrochim. Acta Part A Mol. Biomol. Spectrosc.*, vol. 129, pp. 320–325, Aug. 2014.

[112] W. L. A. Brooks and B. S. Sumerlin, “Synthesis and Applications of Boronic Acid-Containing Polymers: From Materials to Medicine,” *Chem. Rev.*, vol. 116, no. 3, pp. 1375–1397, Feb. 2016.

[113] S. S. Lok, E. Smith MBChB, H. M. Doran, R. Sawyer, N. Yonan, and J. J. Egan, “Idiopathic Pulmonary Fibrosis and Cyclosporine,” *Dan Med Bull*, vol. 29, pp. 27–32, 1998.

[114] S. Groves et al.., “Inhaled cyclosporine and pulmonary function in lung transplant recipients.,” *J. Aerosol Med. Pulm. Drug Deliv.*, vol. 23, no. 1, pp. 31–9, Feb. 2010.

[115] N. Boisa, N. Elom, J. R. Dean, M. E. Deary, G. Bird, and J. A. Entwistle, “Development and application of an inhalation bioaccessibility method (IBM) for lead in the PM10 size fraction of soil,” *Environ. Int.*, vol. 70, pp. 132–142, Sep. 2014.

[116] A. LUDWIG, “The use of mucoadhesive polymers in ocular drug delivery,” *Adv. Drug Deliv. Rev.*, vol. 57, no. 11, pp. 1595–1639, Nov. 2005.

[117] V. Racaniello, “Viruses and the respiratory tract,” *Virology*, 2009. [Online]. Available: http://www.virology.ws/2009/05/21/viruses-and-the-respiratory-tract/. [Accessed: 30-Jul-2017].

[118] S. Clancy, “Genetics of the Influenza Virus,” *Nat. Educ.*, vol. 1, no. 1, p. 83, 2008.